Available online at www.scholarsresearchlibrary.com

Scholars Research Library

Der Pharmacia Lettre, 2012, 4 (4):1246-1269
(http://scholarsresearchlibrary.com/archive.html)

ISSN 0975-5071
USA CODEN: DPLEB4

Quantitative structure activity relationship (QSAR) of cardiac glycosides: the development of predictive *in vitro* cytotoxic activity model

Amitha Joy and Md. Afroz Alam

Department of Biotechnology, Sahrdaya College of Engineering and Technology, Kodakara-680684, Thrissur, India

---

ABSTRACT

Cardiac glycosides are group of natural products found to be effective against various cancers. The aim of this study is to propose a binding mode for different conformation of cardiac glycoside analogues to Na^+, K^+ - ATPase pump which is an important target for various cancer cell lines. Quantitative structure activity relationships model were developed with the cytotoxic activity (Expt. IC_{50}) of 19 compounds based on molecular descriptors like docking score, binding free energy, ADME properties, eMBRAcE solvation model, and pharmacophore based 3D QSAR. In the cases of docking score and binding free energy, the correlation coefficient (R^2) was in the range of 0.65–0.98 indicating good data fit, cross validation coefficient (q^2) in the range of 0.64-0.99 and RMSE was in the range of 0.00–0.36 indicating that the predictive capabilities of the models were acceptable. The prediction model developed for the 226 conformers using docking score and binding free energy showed R^2 in the range of 0.70-0.71, q^2 in the range of 0.69-0.71 and RMSE in the range of 0.22-0.28 indicating acceptable prediction capabilities. In addition, a linear correlation was observed between the predicted and experimented pIC_{50} based on ADME properties with R^2 of 0.88, and q^2 of 0.73 and RMSE = 0.32. The prediction model developed for 226 conformers using ADME properties indicated a better fit with R^2=0.99, q^2= 0.99 and RMSE = 0.28. Further the prediction model developed using liaison showed, R^2=0.90, q^2=0.86, and RMSE=0.23; R^2=0.59, q^2=0.34 and RMSE= 0.45 for original and conformers respectively showing good to non linear response. The prediction model developed using eMBRAcE showed R^2= 0.82, q^2= 0.79 and RMSE= 0.28; R^2= 0.89, q^2= 0.89 and RMSE= 0.20 for original and conformers justify the solvation model parameters are good to use. Finally all the models were validate by pharmacophore based 3D QSAR model for the 19 cardiac glycosides in which the best hypothesis generated correlation coefficient, R^2 =0.9733 which is acceptable pharmacophore features . Low level of RMSE and significant R^2 and q^2 values between Expt. IC_{50} and Predicted IC_{50} revealed that the best quality fit based upon all above said approach.

Keywords: ADME, binding free energy, docking, eMBRAcE, liaison, prediction model

---

INTRODUCTION

1.1 Cardiac glycosides

Cardiac glycosides are a group of natural products occurring in a limited number of plant families and are characterized by their ability to inhibit membrane-bound sodium-potassium activated ATPase [5]. Their continued efficacy in treatment of congestive heart failure and as anti-arrhythmic agents is well appreciated. Less well known however, is the emerging role of this category of compounds in the prevention and /or treatment of proliferative diseases such as cancer [11]. From an ethnopharmacological perspective it may be noted that leaves of *Digitalis purpurea* (containing digoxin) have been used traditionally to treat tumors in different parts of the world [5]. Digitalis glycosides are one of the most useful groups of drugs in therapeutics [10]. The pharmacodynamic properties of digitalis glycosides include inotropic effect, chronotropic effect and toxic and/or side effects [2]. In contrast, it is used for the treatment of heart failure, preclinical and retrospective patient data suggest that cardiac

glycosides (eg. digoxin, digitoxin and ouabain) may reduce the growth of various cancers including breast, lung, prostate, and leukemia [16]. Interstingly several reports indicate that malignant cells are more susceptible to the effects of cardiac glycosides compared to normal cells [5].

The present work created a compound library of cardiac glycosides. Further, prediction models for predicting the cytotoxic activity of these compounds and their conformers were developed based on binding energy, docking score, ADME, eMBrAcE and Linear interaction energy as descriptors. These prediction models were used for predicting the cytotoxic activity of newly developed analogues. ADME model produces a list of 44 descriptors related to absorption, distribution, metabolism and excretion. eMBrAcE calculates ligand-receptor binding energies by molecular mechanics energy minimization of the complex and the separated receptor and ligand, with or without continuum solvation. Linear interaction energy model calculates ligand-receptor binding affinities using a linear interaction approximation.

The antigen-binding fragments (Fabs) of sheep anti-digoxin antibodies (Abs) are used as antidotes for digoxin overdoses [4]. It has been shown that the binding sites of anti-digoxin monoclonal antibody and enzyme are similar [4]. Digoxin is able to occupy the 40-50 Fab sites without major structural rearrangement in either Fab and suggest that the position of digoxin in the 40-50-digoxin complex is likely to be similar to that of ouabain in the ouabain 40-50-ouabain complex [7].

MATERIALS AND METHODS

2.1 Sketching the structure using ISIS Draw

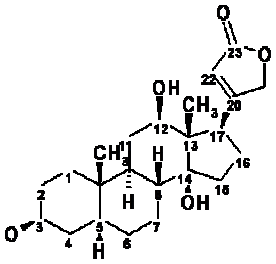

Table 1 Structural features of cardiac glycosides.

Sr. No	Analogues	1	3	5	16	19	Rel inh
1	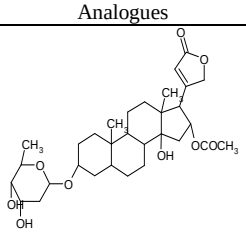 16-acetylgitoxin		Tri-D-digitoxose		$-OCOCH_3$		0.65 ± 0.08
2	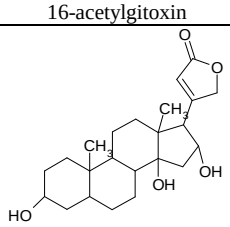 Gitoxigenin		-OH		-OH		1 ± 0.004
3	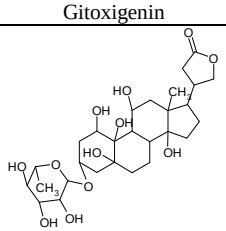 Dihydroouabain	-OH	L-rhamnose	-OH		-OH	1.7 ± 0.1

4	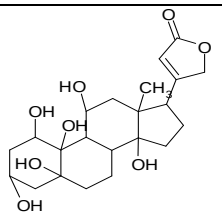 Ouabagenin	-OH	-OH	-OH		-OH	1.6 ± 0.07
5	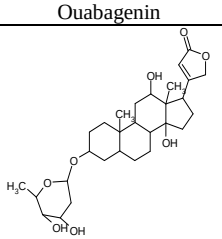 α-acetyldigoxin		Tri-D-digitoxose	Digoxigenin base	-OH		1.4 ± 0.005
6	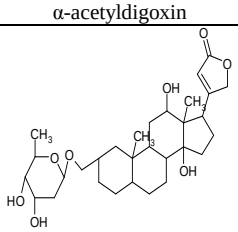 Digoxigenin Bis-digitoxose		Bis-D-digitoxose	Digoxigenin base	-OH		0.63 ± 0.06
7	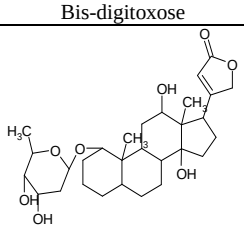 Digoxigenin mono-digitoxose		D-digitoxose	Digoxigenin base	-OH		0.44 ± 0.02
8	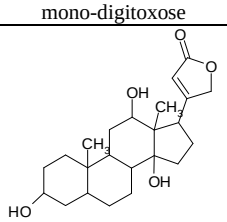 Digoxigenin		-OH	Digoxigenin base	-OH		0.78 ± 0.13
9	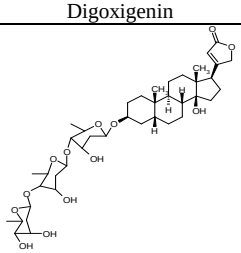 Digitoxin		Tri-D-digitoxose	Digitoxigenin base			0.24 ± 0.04
10	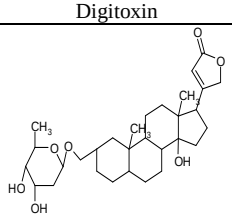 Digitoxigenin bis -digitoxose		Bis-D-digitoxose	Digitoxigenin base			0.15 ± 0.01

11	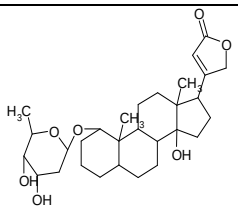 Digitoxigenin mono -digitoxose		D-digitoxose	Digitoxigenin base			0.22 ± 0.02
12	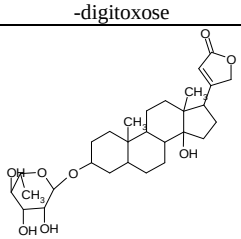 Evomonoside		L-rhamnose	Digitoxigenin base			0.099 ± 0.005
13	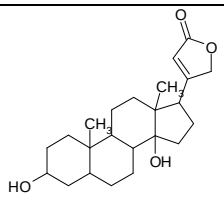 Digitoxigenin		-OH	Digitoxigenin base			0.18 ± 0.02
14	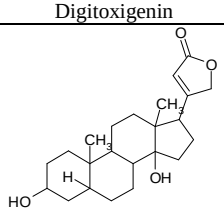 Uzarigenin		-OH	α-H			0.76 ± 0.05
15	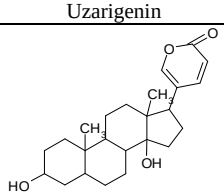 Bufalin		-OH				0.034 ± 0.004
16	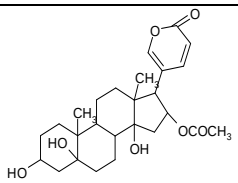 Cinobufagin		-OH	-OH	$OCOCH_3$		0.14 ± 0.004
17	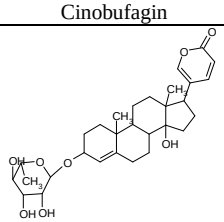 Proscilaridin		L-rhamnose	4-5 double bond			0.13 ± 0.002
18	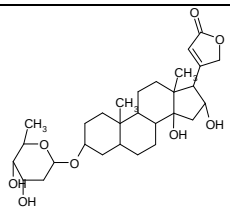 Gitoxin		Tri-D-digitoxose		-OH		2.2 ± 0.2

19	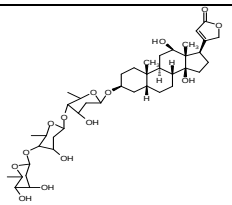 Digoxin		Tri-D-digitoxose	Digoxigenin base	-OH		1 ± 0.1

2.2 Ligand preparation and conformer generation

The sketched structures were first energy minimized using Impact. Impact stands for Integrated modeling program using applied chemical theory. LigPrep (Schrodinger, 2009) has to be used for final preparation of ligands and their conformer (as a control) from individual set of cardiac glycosides and finally generate various conformations libraries for docking insight into the Na^+/K^+-ATPase.

2.3 Receptor preparation

The X-ray structure of the steroid-like compounds designated cardiac glycosides includes well-known drugs as digoxin (PDB ID, 1IGJ) has been used as initial structure in the preparation of cardiac glycosides binding site [12].

2.4 Computational screening based on docking and rescoring function

Molecular docking is a key tool in structural molecular biology and computer-assisted drug design. The goal of ligand—protein docking is to predict the predominant binding mode(s) of a ligand with a protein of known three-dimensional structure. Successful docking methods search high-dimensional spaces effectively and use a scoring function that correctly ranks candidate dockings [13]. The Schrodinger Glide program version 4.0 has to be used for docking (Schrodinger, 2009) for all conformation using Glide in single precision mode (Glide SP). For each screened ligand, the pose with the lowest Glide SP score has been taken as the input for the Glide calculation in extra precision mode (Glide XP). Thus Glide offers the full docking solution for virtual screening from HTVS to SP to XP.

2.5 Computational screening based on mm/gbsa calculation

Combinations of the docking method with other methods, such as MD simulation, free energy binding calculation, enable to get a lot of insights on biological systems and to help rational drug design.

2.6 Computational screening based on embrace approach

The eMBrAcE program (MacroModel v9. 1) program calculates binding energies between ligands and receptors using molecular mechanics energy minimization for docked conformations. eMBrAcE developed by Schrodinger was used for the physics-based rescoring procedure [6].

2.7 Computational screening based on ADME properties

QikProp is a quick, accurate, easy-to-use absorption, distribution, metabolism, and excretion (ADME) prediction program designed by Professor William L. Jorgensen [3]. QikProp predicts physically significant descriptors and pharmaceutically relevant properties of organic molecules, either individually or in batches.

2.8 Pharmacophore based 3D QSAR prediction model

The aim of QSAR study will be to derive a correlation between the biological activity of a set of molecules and their Pharmacophore based descriptor (3D arrangement of an atom into the receptor site).

2.9 Validation of the QSAR model

The predictive capability of the QSAR equation was determined using leave-one out cross validation method. The cross validation regression coefficient (q^2_{cv}) was calculated by the following equation.

$$q^2_{cv} = 1 - \frac{PRESS}{TOTAL} = 1 - \frac{\sum_{i=1}^{n}\left(y_{exp} - y_{pred}\right)^2}{\sum_{i=1}^{n}\left(y_{exp} - \bar{y}\right)^2}$$

where, y_{pred}, y_{exp} and are the predicted, experimental and mean values of experimental activity, respectively. Also the accuracy of the prediction of the QSAR equation was validated by *F*-value and r^2. It has been shown that a high value of statistical characteristics is not necessary for the proof of a highly predictive model [14].

RESULTS AND DISCUSSION

3. 1 Molecular docking of cardiac glycosides

Understanding the mechanisms of enzyme action presents a major challenge and requires the identification of sites that bind Na^+, K^+-ATPase pump [9]. The 19 cardiac glycosides chosen for the present study were systematically docked into the binding sites of the receptor to study the molecular basis of interaction and affinity of binding. This identified the aminoacids that are involved with the binding of cardiac glycosides and the inhibition of ATPase activity. Results of docking showed that Glide determined the optimal orientation of the docked inhibitor, digoxin to be close to that of the original orientation found in the crystal. The low RMS deviation between the docked and crystal ligand coordinates indicate very good alignment of the experimental and calculated positions especially considering the resolution of the crystal structure ($2.5A^0$). The ligand binding residues involved in the ligand interactions and the hydrogen bond interactions of 6 configurations are shown in Figure 2. For each ligand, the pose with the lowest Glide score was rescored using Prime/MM-GBSA approach. This approach is used to predict the binding free energy (ΔG_{bind}) for set of ligands to the receptor.

Table 2 Docking score and RMSD from the docking simulation of cardiac glycosides in the receptor protein.

Compounds	Dock Score	ΔG^a score	RMSD^b (A^0)	ΔRMD^c (A^0)	Compounds	Dockscore	ΔG^a score	RMSD^b (A^0)	ΔRMSD^c (A^0)
Ouabagenin.	-11.47	0	0.0007	0.00	Gitoxigenin	-9.72	-0.1	0.001	0.009
Ouabain	-11.30	-0.17	0.03	-0.0293	Digoxigenin bis-digitoxose	-9.68	-0.04	0.02	-0.019
Dihydroouabain	-11.04	-0.26	0.01	0.02	Cinobufagin	-9.56	-0.12	0.009	0.011
Proscillaridin	-10.55	-0.49	0.009	0.01	Digoxigenin	-9.02	-0.54	0.04	-0.031
Digoxigenin monodigitoxose	-10.42	-0.13	0.003	0.006	Evomonoside	-8.80	-0.21	0.04	0.00
Digoxin	-10.33	-0.09	0.04	-0.037	Digitoxin	-8.64	-8.80	0.01	0.03
Digitoxigenin bis-digitoxose	-10.14	-0.19	0.002	0.038	Bufalin.1	-6.82	8.64	0.003	0.007
Alphaacetyldigoxin	-10.04	-0.1	0.003	-0.001	Uzarigenin.1	-6.80	-1.82	0.006	-0.003
16-acetylgitoxin	-9.82	-0.22	0.01	-0.007	Digitoxigenin.	-6.69	-0.02	0.003	0.003
Gitoxin	-9.82	0	0.01	0.00					

[a]DGscore=Ei-Elowest, [b]RMSD RMSD between docked and crystallographic structure, [c]RMSD, RMSD between docked poses corresponding to each configuration

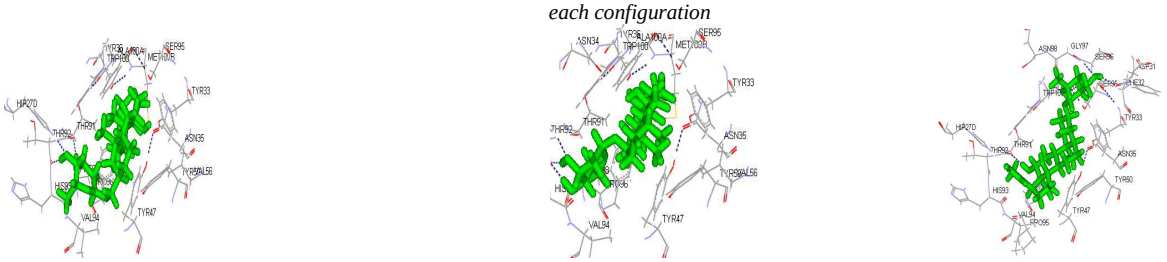

Digitoxigenin-bis-digitoxose
Docking score= -10.14
Binding energy= -26.64
RMSD=0.002

Alphaacetyldigoxin
Docking score= -10.04
Binding energy= -42.64
RMSD= 0.003

Digoxigenin-mono- digitoxose
Docking score= -10.42
Binding energy= -29.99
RMSD=0.003

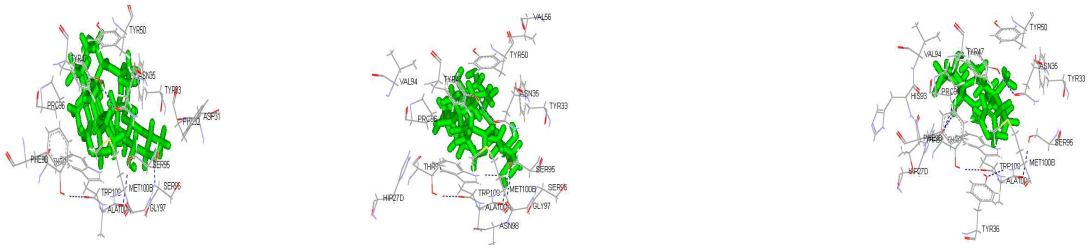

Digoxin
Docking score=-10.33
Binding energy=-41.46
RMSD=0.04

Dihydroouabain
Docking score= -11.04
Binding energy=-51.70
RMSD= 0.01

Ouabagenin
Docking score=-11.47
Binding energy=-33.26
RMSD=0.0007

Fig 1. Binding site residues and hydrogen bond interactions

3.2 Cytotoxicity prediction model based on docking score and ΔG binding

Ligands with known experimental activity (IC_{50}) were selected based on the relative inhibition values of cardiotonic steroids for sheep kidney Na^+, K^+-ATPase. Because digoxin is the cardiotonic agent most widely used in the United States, it served as the reference compound and the observed rel inh values (IC_{50} values relative to digoxin) for all the compounds [4] presented in Table 1. The therapeutic effect of cardiac glycosides lies in their reversible inhibition on the membrane bound Na^+,K^+-ATPase located in human myocardium [15]. Thus in this study we have taken the murine anti-digoxin monoclonal antibody (mAb) 26-10 as the molecular target since it is previously shown that the environment of the binding sites of the 26-10 and the enzyme are similar [4]. We have built prediction model for prediction of cytotoxic activity by considering the Glide score as descriptor. The equation of the model and the corresponding statistics are shown below.

$$pIC_{50}= -2.78\ (\pm0.008)-0.357(\pm0.453)*\text{Docking Score}$$

DF=18, R^2=0.6582, S=0.5676, F=6.05, P=0.05, PRESS=6.52464, r^2cv=0.64, RMSE=0.36

The quality of the fit can be judged by the value of the squared correlation coefficient (R^2), which was 0.6582 for the data set. The statistical significance of the prediction model is evaluated by the correlation coefficient R^2, standard error, F-test value, leave-one-out cross-validation coefficient R^2_{cv} and predictive error sum of squares PRESS. Prime/MM-GBSA protocol was used for rescoring Glide XP poses of the cardiac glycosides. A high correlation was found between ΔG_{bind} energy and experimental pIC_{50}. Rescoring using Prime/MM-GBSA leads to minor changes of the ligand conformations (due to energy minimization of the ligand in receptor's environment) and consequent stabilization of receptor and ligand complex. A linear regression model for prediction of predicted pIC_{50} of cytotoxicity has been developed by considering some analogues with known pIC_{50}. In this model we have taken ΔG_{bind} energy as a descriptor. The equation of the model and the corresponding statistics are shown below.

$$pIC_{50}= -2.78\ (\pm0.1)-0.0230(\pm0.45)*\Delta G$$

DF=18, R^2=0.9897, s=0.6233, PRESS=8.17839, F=4.35, P=0.001, r^2cv=0.99, RMSE=0

The RMSE value between the experimental and predicted free energy of binding values was 0 which is comparable to the level of accuracy achieved by the most accurate methods such as free energy perturbation. This agrees with the analysis methodology adopted by Alam et. al., 2008.

Table 3 Predicted cytotoxic activities of cardiac glycosides analogues based on docking score and Prime/MM-GBSA energy

Sr. No.	Compounds	Docking score	Prime MMGBSA ΔG bind	Expt. IC_{50}	Pred. IC_{50}	Pred. IC_{50}
1	Digoxigenin bis-digitoxose	-9.68	-33.75	0.63	0.61	0.65
2	Digoxigenin monodigitoxose	-10.42	-29.99	0.44	0.47	0.46
3	Digitoxigenin	-8.79	-34.81	0.18	0.20	0.17
4	Digitoxin	-9.34	-46.19	0.24	0.19	0.24
5	Digitoxigenin bis-digitoxose	-10.14	-26.64	0.15	0.17	0.17
6	Evomonoside	-8.81	-24.37	0.10	0.14	0.12
7	Cinobufagin	-9.56	-48.10	0.14	0.17	0.16
8	Bufalin	-9.03	-37.48	0.03	0.04	0.03
9	Proscillaridin	-10.55	-42.10	0.13	0.13	0.12
10	16-acetylgitoxin	-9.82	-36.75	0.65	0.66	0.72
11	Dihydroouabain	-11.04	-51.70	1.7	1.85	1.70
12	Ouabain	-11.30	-46.03	1	1.13	0.96
13	Ouabagenin	-11.47	-33.26	1.6	1.24	1.64
14	Digoxin	-10.33	-41.46	1	0.99	0.86
15	Gitoxigenin	-9.72	-40.34	1	0.99	1.00
16	Gitoxin	-9.82	-36.75	2.2	0.66	2.17
17	Uzarigenin	-8.59	-36.20	0.76	0.72	0.70
18	Digoxigenin	-9.08	-32.84	0.78	0.79	0.63
19	Alphaacetyldigoxin	-10.04	-42.64	1.4	1.39	1.53

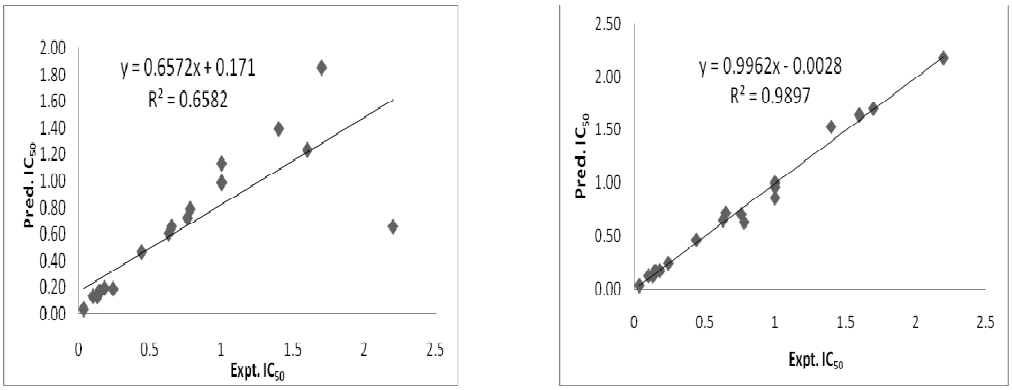

Figure 2. Models for predicting cytotoxic activity (pIC_{50}) of the cardiac glycosides analogues based on Glide score and Prime/MM-GBSA energy

Table 4 Predicted cytotoxic activities of cardiac glycosides conformers based on Docking Score.

Compounds	Dock Score	Expt. IC_{50}	Pred. IC_{50}	Compounds	Dock Score	Expt. IC_{50}	Pred. IC_{50}
DB- C1	-9.60	0.61	0.33	BU-C21	-6.10	0.04	0.31
DB- C2	-9.38	0.61	0.72	BU-C3	-8.26	0.04	0.08
DB--C3	-9.36	0.61	0.71	BU-C4	-8.19	0.04	0.07
DB--C4	-9.36	0.61	0.71	BU-C5	-8.15	0.04	0.04
DB-C5	-9.01	0.61	0.67	BU-C6	-8.02	0.04	0.05
DB- C6	-8.74	0.61	0.64	BU-C7	-8.01	0.04	0.05
DB- C7	-8.27	0.61	0.58	BU-C8	-7.97	0.04	0.04
DB- C8	-8.18	0.61	0.57	BU-C9	-7.95	0.04	0.04
DB- C9	-8.05	0.61	0.55	PR-C1	-9.34	0.13	0.01
DM-C1	-9.56	0.47	0.74	PR-C10	-8.05	0.13	0.12
DM-C2	-9.10	0.47	0.68	PR-C11	-8.01	0.13	0.12
DM-C3	-8.90	0.47	0.66	PR-C12	-7.98	0.13	0.13
DM-C4	-8.13	0.47	0.56	PR-C13	-7.95	0.13	0.13
DT-C1	-8.53	0.2	0.61	PR-C14	-7.95	0.13	0.13
DT-C10	-7.63	0.2	0.50	PR-C15	-7.94	0.13	0.13
DT-C11	-7.63	0.2	0.50	PR-C16	-7.93	0.13	0.13
DT-C12	-7.56	0.2	0.49	PR-C17	-7.93	0.13	0.12
DT-C13	-7.54	0.2	0.49	PR-C18	-7.91	0.13	0.12
DT-C14	-7.50	0.2	0.49	PR-C19	-7.90	0.13	0.12
DT-C15	-7.45	0.2	0.48	PR-C2	-8.90	0.13	0.12
DT-C16	-7.41	0.2	0.47	PR-C20	-7.89	0.13	0.14
DT-C17	-7.36	0.2	0.47	PR-C21	-7.86	0.13	0.14
DT-C18	-7.22	0.2	0.45	PR-C22	-7.85	0.13	0.14
DT-C19	-7.22	0.2	0.45	PR-C23	-7.83	0.13	0.14
DT-C2	-8.39	0.2	0.59	PR-C24	-7.81	0.13	0.14
DT-C20	-7.20	0.2	0.45	PR-C25	-7.79	0.13	0.12
DT-C21	-6.69	0.2	0.39	PR-C26	-7.78	0.13	0.12
DT-C22	-6.44	0.2	0.36	PR-C27	-7.75	0.13	0.12
DT-C23	-6.22	0.2	0.33	PR-C28	-7.72	0.13	0.12
DT-C3	-8.29	0.2	0.58	PR-C29	-7.68	0.13	0.12
DT-C4	-8.17	0.2	0.57	PR-C3	-8.72	0.13	0.12
DT-C5	-8.07	0.2	0.56	PR-C30	-7.65	0.13	0.12
DT-C6	-8.02	0.2	0.55	PR-C31	-7.62	0.13	0.12
DT-C7	-7.89	0.2	0.53	PR-C4	-8.43	0.13	0.12
DT-C8	-7.81	0.2	0.52	PR-C5	-8.31	0.13	0.12
DT-C9	-7.70	0.2	0.51	PR-C6	-8.25	0.13	0.14
DG-C1	-8.64	0.19	0.63	PR-C7	-8.08	0.13	0.14
DG-C2	-8.26	0.19	0.58	PR-C8	-8.06	0.13	0.14
DG-C3	-7.43	0.19	0.48	PR-C9	-8.05	0.13	0.14
DG-C4	-7.41	0.19	0.47	AG-C1	-8.61	0.66	0.62
DG-C5	-5.94	0.19	0.29	AG-C2	-8.37	0.66	0.59
DG-C6	-5.91	0.19	0.29	AG-C3	-8.34	0.66	0.59
TB-C1	-9.61	0.17	0.17	AG-C4	-8.02	0.66	0.55
TB- C10	-8.50	0.17	0.61	AG-C5	-7.92	0.66	0.54
TB- C11	-8.24	0.17	0.58	DH-C1	-9.95	1.85	0.79
TB-C12	-7.84	0.17	0.53	OU-C1	-10.73	1.13	1.15
TB- C13	-7.71	0.17	0.16	OU-C2	-10.69	1.13	1.15
TB- C2	-9.58	0.17	0.18	OU-C3	-10.46	1.13	1.14
TB- C3	-9.53	0.17	0.18	OU-C4	-10.25	1.13	1.15

TB- C4	-9.37	0.17	0.17	OB-C1	-10.53	1.24	1.25
TB- C5	-9.15	0.17	0.69	OB-C10	-8.65	1.24	1.25
TB- C6	-9.10	0.17	0.68	OB-C2	-9.81	1.24	1.25
TB- C7	-9.07	0.17	0.16	OB-C3	-9.67	1.24	1.25
TB- C8	-8.95	0.17	0.17	OB-C4	-9.41	1.24	1.25
TB- C9	-8.59	0.17	0.62	OB-C5	-9.22	1.24	1.25
EV-C1	-8.47	0.14	0.13	OB-C6	-9.18	1.24	1.25
EV-C2	-6.29	0.14	0.34	OB-C7	-8.87	1.24	1.25
EV-C3	-6.11	0.14	0.31	OB-C8	-8.67	1.24	1.25
CI-C1	-8.96	0.17	0.66	OB-C9	-8.65	1.24	1.25
CI-C2	-8.75	0.17	0.64	DI-C1	-9.83	0.99	0.77
CI-C3	-8.20	0.17	0.57	DI-C10	-7.27	0.99	0.46
CI-C4	-7.87	0.17	0.53	DI-C11	-5.89	0.99	0.98
CI-C5	-4.96	0.17	0.17	DI-C12	-5.81	0.99	0.98
BU-C1	-8.37	0.04	0.59	DI-C2	-9.73	0.99	0.98
BU-C10	-7.89	0.04	0.53	DI-C3	-9.40	0.99	0.98
BU-C11	-7.84	0.04	0.53	DI-C4	-8.89	0.99	0.98
BU-C12	-7.78	0.04	0.52	DI-C5	-8.66	0.99	0.98
BU-C13	-7.73	0.04	0.51	DI-C6	-8.47	0.99	0.98
BU-C14	-7.53	0.04	0.49	DI-C7	-8.35	0.99	0.98
BU-C15	-7.50	0.04	0.49	DI-C8	-8.31	0.99	0.98
BU-C16	-7.33	0.04	0.46	DI-C9	-8.19	0.99	0.98
BU-C17	-7.27	0.04	0.06	GI-C1	-8.98	0.99	0.98
BU-C18	-7.04	0.04	0.03	GI-C10	-7.93	0.99	0.98
BU-C19	-6.98	0.04	0.03	GI-C11	-7.88	0.99	0.98
BU-C2	-8.36	0.04	0.05	GI-C12	-7.87	0.99	0.98
BU-C20	-6.82	0.04	0.40	GI-C13	-7.84	0.99	0.99
GI-C16	-7.69	0.99	0.99	GI-C14	-7.79	0.99	0.99
GI-C17	-7.69	0.99	0.99	GI-C15	-7.77	0.99	0.99
GI-C18	-7.64	0.99	0.99	DN-C10	-7.35	0.79	0.47
GI-C19	-7.45	0.99	0.99	DN-C11	-7.25	0.79	0.46
GI-C2	-8.81	0.99	0.99	DN-C12	-7.24	0.79	0.45
GI-C20	-7.25	0.99	0.99	DN-C13	-7.23	0.79	0.45
GI-C21	-6.97	0.99	0.99	DN-C14	-7.20	0.79	0.45
GI-C22	-6.09	0.99	0.99	DN-C15	-7.10	0.79	0.44
GI-C3	-8.72	0.99	0.99	DN-C16	-7.07	0.79	0.43
GI-C4	-8.30	0.99	0.99	DN-C17	-6.93	0.79	0.42
GI-C5	-8.29	0.99	0.99	DN-C18	-6.84	0.79	0.40
GI-C6	-8.19	0.99	0.99	DN-C19	-6.84	0.79	0.40
GI-C7	-8.18	0.99	0.99	DN-C2	-8.76	0.79	0.64
GI-C8	-8.08	0.99	0.99	DN-C3	-8.33	0.79	0.59
GI-C9	-8.00	0.99	0.99	DN-C4	-7.89	0.79	0.53
GT-C1	-8.61	0.66	0.62	DN-C5	-7.89	0.79	0.53
GT-C2	-8.37	0.66	0.59	DN-C6	-7.79	0.79	0.52
GT-C3	-8.34	0.66	0.59	DN-C7	-7.75	0.79	0.52
GT-C4	-8.02	0.66	0.55	DN-C8	-7.65	0.79	0.50
GT-C5	-7.92	0.66	0.54	DN-C9	-7.41	0.79	0.47
UZ-C1	-8.46	0.72	0.60	AD-C1	-9.64	1.39	1.41
UZ-C10	-7.63	0.72	0.50	AD-C2	-8.98	1.39	1.41
UZ-C11	-7.61	0.72	0.50	AD-C3	-8.57	1.39	1.41
UZ-C12	-7.60	0.72	0.50	AD-C4	-8.53	1.39	1.41
UZ-C13	-7.60	0.72	0.50	AD-C5	-8.53	1.39	1.40
UZ-C14	-7.58	0.72	0.49	AD-C6	-8.28	1.39	1.40
UZ-C15	-7.50	0.72	0.49	AD-C7	-8.12	1.39	1.40
UZ-C16	-7.38	0.72	0.47	AD-C8	-7.85	1.39	1.40
UZ-C17	-7.37	0.72	0.47	AD-C9	-7.54	1.39	1.40
UZ-C18	-7.31	0.72	0.46	UZ-C20	-6.88	0.72	0.41
UZ-C19	-7.31	0.72	0.46	UZ-C21	-6.80	0.72	0.40
UZ-C2	-8.44	0.72	0.60	UZ-C22	-6.76	0.72	0.39
UZ-C23	-6.61	0.72	0.38	UZ-C6	-8.22	0.72	0.57
UZ-C24	-6.47	0.72	0.36	UZ-C7	-7.90	0.72	0.53
UZ-C3	-8.35	0.72	0.59	UZ-C8	-7.80	0.72	0.52
UZ-C4	-8.33	0.72	0.59	UZ-C9	-7.74	0.72	0.52
UZ-C5	-8.22	0.72	0.57	DN-C1	-9.02	0.79	0.67

dm-digoxigeninmonodigitoxose, db-digoxigeninbisdigitoxose, dt-digitoxigenin, bu-bufalin, ev evomonoside, di-digoxin, ci-cinobufagin, dn-digoxigenin, uz-uzarigenin, pr-proscillaridin, dg-digitoxin, gi-gitoxigenin, gt-gitoxin, ag-16-acetylgitoxin, ou-ouabain, ob-ouabagenin, dh-dihydroouabain, tb- digitoxigenin bis digitoxose, ad-alphaacetyldigoxin

The prediction models for prediction of cytotoxic activity of the conformers were also built by considering the Glide score as descriptor. A better correlation was found between Glide GSscore and experimental pIC_{50} for conformers. The equation of the thermomodel and the corresponding statistics are shown below.

$$pIC_{50} = - 0.437 (\pm0.23) - 0.123 (\pm0.36) * \text{Docking Score}$$

DF=225, PRESS=38.1647, S=0.4091, R^2=0.717, F=16.96, P=0.001, r^2cv=0.71, RMSE=0.22

The prediction models for prediction of cytotoxic activity of the conformers were built by considering the Prime/MM-GBSA as descriptor. The equation of the thermomodel and the corresponding statistics are shown below.

$$pIC_{50} = 0.246 (\pm0.52) - 0.00870 (\pm0.43)*\Delta G$$

DF=225, F=3.91, P=0.05, R^2=0.7025, PRESS=60.4502, r^2cv=0.69, RMSE=0.28

Table 5 Predicted cytotoxic activities of cardiac glycosides conformers using Prime/MM-GBSA energy as a descriptor and experimental activity values

Compounds	ΔG	Expt. IC_{50}	Pred. IC_{50}	Compounds	ΔG	Expt.IC_{50}	Pred. IC_{50}
DB -C1	-40.74	0.65	0.60	PR-C27	-40.88	0.12	0.12
DB -C2	-24.80	0.65	0.46	PR-C28	-40.99	0.12	0.12
DB-C3	-34.19	0.65	0.54	PR-C29	-40.60	0.12	0.12
DB -C4	-19.81	0.65	0.42	PR-C3	-44.93	0.12	0.12
DB -C5	-23.61	0.65	0.45	PR-C30	-45.29	0.12	0.12
DB -C6	-32.02	0.65	0.52	PR-C31	-41.90	0.12	0.12
DB -C7	-25.28	0.65	0.47	PR-C4	-58.57	0.12	0.12
DB -C8	-36.44	0.65	0.56	PR-C5	-42.55	0.12	0.12
DB-C9	-30.03	0.65	0.51	PR-C6	-41.61	0.12	0.12
DM-C1	-41.05	0.46	0.60	PR-C7	-46.25	0.12	0.12
DM -C2	-42.27	0.46	0.61	PR-C8	-45.80	0.12	0.64
DM-C3	-43.89	0.46	0.63	PR-C9	-36.15	0.12	0.56
DM-C4	-51.34	0.46	0.69	AG-C1	-42.97	0.72	0.62
DT-C1	-36.67	0.17	0.57	AG-C2	-50.57	0.72	0.69
DT-C10	-34.38	0.17	0.55	AG-C3	-47.95	0.72	0.66
DT-C11	-40.54	0.17	0.60	AG-C4	-37.55	0.72	0.57
DT-C12	-42.56	0.17	0.62	AG-C5	-49.71	0.72	0.68
DT-C13	-36.98	0.17	0.57	DH-C1	-61.29	1.7	0.78
DT-C14	-45.86	0.17	0.65	OU-C1	-44.03	0.96	0.63
DT-C15	-27.81	0.17	0.49	OU-C2	-47.73	0.96	0.66
DT-C16	-31.93	0.17	0.52	OU-C3	-45.82	0.96	0.64
DT-C17	-26.60	0.17	0.48	OU-C4	-52.37	0.96	0.70
DT-C18	-36.90	0.17	0.57	DI-C1	-37.53	0.86	0.57
DT-C19	-32.71	0.17	0.53	DI-C10	-51.33	0.86	0.69
DT-C2	-29.79	0.17	0.51	DI-C11	-39.54	0.86	0.59
DT-C20	-39.62	0.17	0.59	DI-C12	-58.62	0.86	0.76
DT-C21	-39.30	0.17	0.59	DI-C2	-60.35	0.86	0.77
DT-C22	-42.78	0.17	0.62	DI-C3	-23.78	0.86	0.45
DT-C23	-42.70	0.17	0.62	DI-C4	-40.75	0.86	0.60
DT-C3	-43.66	0.17	0.63	DI-C5	-39.63	0.86	0.59
DT-C4	-45.83	0.17	0.64	DI-C6	-40.08	0.86	0.59
DT-C5	-41.34	0.17	0.61	DI-C7	-43.96	0.86	0.63
DT-C6	-36.30	0.17	0.56	DI-C8	-55.56	0.86	0.73
DT-C7	-37.57	0.17	0.57	DI-C9	-59.00	0.86	0.76
DT-C8	-41.31	0.17	0.61	GI-C1	-35.35	1	0.99
DT-C9	-35.63	0.17	0.56	GI-C10	-40.91	1	0.60
OB-C1	-28.59	1.64	1.64	GI-C11	-35.76	1	0.56
OB-C10	-40.59	1.64	1.64	GI-C12	-43.90	1	1.00
OB-C2	-51.08	1.64	1.65	GI-C13	-38.52	1	1.00
OB-C3	-47.36	1.64	1.65	GI-C14	-39.85	1	1.00
OB-C4	-42.99	1.64	1.65	GI-C15	-38.52	1	1.00
OB-C5	-35.03	1.64	1.65	GI-C16	-37.99	1	1.00
OB-C6	-52.11	1.64	1.65	GI-C17	-49.11	1	0.67
OB-C7	-41.25	1.64	1.64	GI-C18	-24.96	1	0.46
OB-C8	-45.68	1.64	1.64	GI-C19	-33.64	1	1.00
OB-C9	-38.90	1.64	1.64	GI-C2	-27.25	1	0.48
CI-C1	-53.09	0.16	0.16	GI-C20	-38.58	1	0.58
CI-C2	-17.12	0.16	0.16	GI-C21	-33.45	1	1.00
CI-C3	-35.95	0.16	0.16	GI-C22	-40.17	1	1.00
CI-C4	-43.37	0.16	0.16	GI-C3	-45.10	1	1.00
CI-C5	-36.21	0.16	0.16	GI-C4	-37.05	1	1.00
EV-C1	-41.18	0.12	0.13	GI-C5	-36.12	1	1.00
EV-C2	-36.58	0.12	0.13	GI-C6	-34.72	1	1.00
EV-C3	-26.98	0.12	0.13	GI-C7	-35.12	1	1.00
TB--C1	-27.82	0.17	0.16	GI-C8	-43.18	1	0.62
TB-C10	-28.18	0.17	0.17	GI-C9	-35.47	1	0.55

TB-C11	-36.39	0.17	0.18	GT-C1	-43.34	2.17	2.16
TB-C12	-33.15	0.17	0.18	GT-C2	-50.57	2.17	2.16
TB-C13	-43.02	0.17	0.18	GaT-C3	-47.95	2.17	2.16
TB- C2	-33.85	0.17	0.18	GT-C4	-37.55	2.17	2.16
TB -C3	-28.27	0.17	0.18	GT-C5	-49.71	2.17	1.68
TB -C4	-32.35	0.17	0.18	UZ-C1	-38.54	0.7	0.58
TB -C5	-47.93	0.17	0.17	UZ-C10	-52.50	0.7	0.70
TB -C6	-28.82	0.17	0.17	UZ-C11	-29.11	0.7	0.50
TB -C7	-33.96	0.17	0.17	UZ-C12	-36.66	0.7	0.56
TB -C8	-36.82	0.17	0.17	UZ-C13	-37.94	0.7	0.58
TB -C9	-36.36	0.17	0.17	UZ-C14	-36.80	0.7	0.57
DG-C1	-46.43	0.24	0.24	UZ-C15	-32.87	0.7	0.53
DG-C2	-49.27	0.24	0.24	UZ-C16	-32.47	0.7	0.53
DG-C3	-47.70	0.24	0.24	UZ-C17	-36.96	0.7	0.57
DG-C4	-52.40	0.24	0.24	UZ-C18	-35.43	0.7	0.55
DG-C5	-46.99	0.24	0.23	UZ-C19	-36.31	0.7	0.56
DG-C6	-37.76	0.24	0.23	UZ-C2	-34.16	0.7	0.54
BU-C1	-39.20	0.03	0.02	UZ-C20	-43.85	0.7	0.63
BU-C10	-41.55	0.03	0.01	UZ-C21	-32.95	0.7	0.53
BU-C11	-43.20	0.03	0.01	UZ-C22	-40.51	0.7	0.60
BU-C12	-27.04	0.03	0.01	UZ-C23	-45.52	0.7	0.64
BU-C13	-32.91	0.03	0.01	UZ-C24	-31.47	0.7	0.52
BU-C14	-34.69	0.03	0.01	UZ-C3	-36.91	0.7	0.57
BU-C15	-38.70	0.03	0.01	UZ-C4	-34.48	0.7	0.55
BU-C16	-26.90	0.03	0.02	UZ-C5	-30.94	0.7	0.52
BU-C17	-33.03	0.03	0.02	UZ-C6	-48.55	0.7	0.67
BU-C18	-33.43	0.03	0.02	UZ-C7	-37.14	0.7	0.57
BU-C19	-30.33	0.03	0.02	UZ-C8	-36.35	0.7	0.56
BU-C2	-44.92	0.03	0.02	UZ-C9	-24.10	0.7	0.46
BU-C20	-35.09	0.03	0.02	DN-C1	-44.87	0.63	0.64
BU-C21	-24.05	0.03	0.02	DN-C10	-39.37	0.63	0.59
BU-C3	-41.81	0.03	0.02	DN-C11	-42.85	0.63	0.62
BU-C4	-39.45	0.03	0.02	DN-C12	-34.87	0.63	0.55
BU-C5	-27.10	0.03	0.02	DN-C13	-47.54	0.63	0.66
BU-C6	-41.18	0.03	0.02	DN-C14	-27.82	0.63	0.49
BU-C7	-31.46	0.03	0.02	DN-C15	-34.13	0.63	0.54
BU-C8	-31.12	0.03	0.02	DN-C16	-33.91	0.63	0.54
BU-C9	-26.17	0.03	0.47	DN-C17	-36.58	0.63	0.56
PR-C1	-45.94	0.12	0.12	DN-C18	-29.28	0.63	0.50
PR-C10	-35.08	0.12	0.12	DN-C19	-33.63	0.63	0.54
PR-C11	-43.37	0.12	0.12	DN-C2	-32.73	0.63	0.53
PR-C12	-43.02	0.12	0.12	DN-C3	-36.03	0.63	0.56
PR-C13	-42.96	0.12	0.12	DN-C4	-29.58	0.63	0.50
PR-C14	-43.72	0.12	0.12	DN-C5	-33.72	0.63	0.54
PR-C15	-44.01	0.12	0.12	DN-C6	-48.87	0.63	0.67
PR-C16	-47.05	0.12	0.12	DN-C7	-33.90	0.63	0.54
PR-C17	-44.24	0.12	0.12	DN-C8	-23.40	0.63	0.45
PR-C18	-39.94	0.12	0.12	DN-C9	-41.88	0.63	0.61
PR-C19	-42.20	0.12	0.12	AD-C1	-35.14	1.53	0.55
PR-C2	-62.22	0.12	0.12	AD-C2	-37.30	1.53	0.57
PR-C20	-44.61	0.12	0.63	AD-C3	-40.75	1.53	0.60
PR-C21	-39.31	0.12	0.59	AD-C4	-29.71	1.53	0.50
PR-C22	-39.24	0.12	0.59	AD-C5	-40.01	1.53	0.59
PR-C23	-35.08	0.12	0.55	AD-C6	-32.10	1.53	0.53
PR-C24	-39.18	0.12	0.59	AD-C7	-29.53	1.53	0.50
PR-C25	-42.39	0.12	0.12	AD-C8	-37.68	1.53	0.57
PR-C26	-42.00	0.12	0.12	AD-C9	-41.13	1.53	0.60

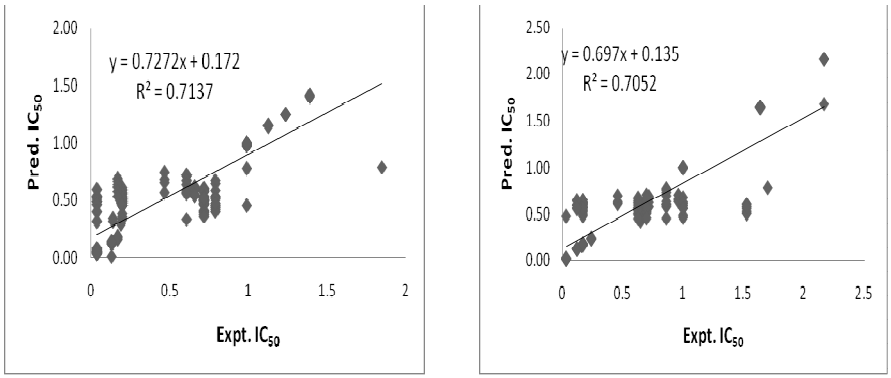

Figure 3. Models for predicting cytotoxic activity (pIC_{50}) of the cardiac glycosides conformers based on Docking score and Prime/MM-GBSA energy

For docking sore and binding energy the R^2 was in the range of 0.6582–0.9897 indicating good data fit and r^2_{cv} was in the range of 0.69-0.99 indicating that the predictive capabilities of the models were acceptable. Relationship between predicted and experimental activities of original set and conformer set as per the QSAR equation. The correlation coefficient (R^2) for both the data set was > 0.65.

3. 2 Cytotoxicity prediction model based on ADME screening

The QikProp program [3] was used to obtain the ADME properties of the analogues. It predicts both physically significant descriptors and pharmaceutically relevant properties. According to the analysis 44 physically significant descriptors and pharmaceutically relevant properties of cardiac glycosides, among which molwt, SASA, FOSA, FISA, PISA, volume, glob, QPpolrz, QPlogPC16, QPlogPoct, QPlogPw, QPlogPo/w, QPlogS, CIQPlogS, QPlogHERG, QPPCaco, QPlogBB were considered for predicting the cytotoxic activity. QPPMDCK, QPlogKp, QPlogKhsa, PercentHumanOralAbsorption and PSA have been removed from the equation, because they are highly correlated with other X variables.

Table 6 Screening of ADME properties for cardiac glycosides using Qiikprop simulation

Sr. No	Compounds	MW	SASA	FOSA	FISA	PISA	Volume	Glob	QPpolrz
1	Digoxigeninbis-digitoxose	534.6	692.2	493.4	176.1	22.6	1457.5	0.90	47.90
2	Digoxigeninmonodigitoxose	520.6	738.2	541.0	184.8	12.4	1476.0	0.85	49.18
3	Digitoxigenin	374.5	589.8	440.8	129.1	19.8	1135.8	0.89	38.21
4	digitoxigeninbis-digitoxose	518.6	746.8	531.5	191.6	23.6	1517.0	0.85	50.93
5	Evomonoside	520.6	751.0	529.3	189.7	31.9	1482.3	0.84	49.62
6	Bufalin	386.5	614.8	398.6	128.5	87.6	1170.8	0.87	40.26
7	Cinobufagin	460.5	680.1	414.2	191.4	74.4	1318.1	0.85	44.74
8	Proscillaridin	530.6	775.9	509.8	182.0	84.0	1527.0	0.83	51.91
9	Digitoxin	764.9	1073.	812.3	230.2	30.6	2154.1	0.75	73.28
10	16-acetylgitoxin	520.6	735.5	513.0	202.8	19.5	1471.1	0.85	49.06
11	Dihydroouabain	572.6	753.5	431.3	322.1	0.00	1509.3	0.84	47.83
12	Ouabain	614.7	847.3	575.8	264.8	6.67	1690.7	0.81	51.94
13	Digoxin	780.9	968.9	703.8	245.8	19.1	2103.1	0.82	70.49
14	Gitoxigenin	390.5	589.7	387.9	181.5	20.2	1147.9	0.90	38.05
15	Gitoxin	520.6	735.5	513.0	202.8	19.5	1471.1	0.85	49.06
16	Uzarigenin	374.5	590.0	442.3	128.5	19.1	1130.7	0.89	38.00
17	Digoxigenin	390.5	592.9	401.0	167.8	24.1	1144.1	0.89	37.94
18	Alphaacetyldigoxin	520.6	764.2	545.5	197.6	21.0	1490.2	0.83	49.83
19	Ouabagenin	424.4	587.8	354.0	222.6	11.1	1139.7	0.90	35.71

QPlogPC16	QPlogPoct	QPlogPw	QPlogPo/w	QPlogS	CIQPlogS	QPlogHERG	QPPCaco	QPlogBB	Expt. IC_{50}	Pred. IC_{50}
13.91	29.54	19.12	2.02	-3.71	-5.23	-3.29	211.5	-1.31	0.63	0.65
14.09	29.56	19.44	1.97	-4.53	-4.97	-4.03	175.1	-1.51	0.44	0.42
10.39	19.38	10.01	3.16	-4.72	-4.74	-3.37	590.2	-0.64	0.18	0.16
14.32	28.55	16.44	2.94	-5.11	-5.63	-3.99	150.8	-1.55	0.15	0.16
14.34	29.66	19.64	1.97	-4.71	-4.97	-4.32	157.3	-1.60	0.10	0.99
11.13	19.82	10.03	3.64	-5.29	-5.30	-3.99	598.2	-0.68	0.03	0.20
12.98	24.78	14.26	2.88	-5.18	-5.65	-4.24	151.3	-1.43	0.14	0.15
15.07	30.12	19.51	2.52	-5.21	-5.60	-4.74	186.2	-1.57	0.13	0.14
21.32	43.37	29.41	1.88	-5.36	-6.41	-5.70	64.95	-2.82	0.24	0.23
14.22	29.82	19.60	1.82	-4.49	-4.97	-4.05	118.1	-1.67	0.65	0.88
16.17	37.93	30.13	-0.98	-3.11	-3.77	-4.05	8.73	-3.05	1.70	1.72
17.73	39.51	31.06	-0.09	-3.19	-4.08	-4.64	30.51	11.38	1.00	1.34

20.28	45.82	32.11	1.12	-4.13	-6.00	-4.55	46.20	-2.60	1.00	1.06
11.12	22.15	13.29	2.10	-4.06	-4.36	-3.26	188.0	-1.12	1.00	1.32
14.22	29.82	19.60	1.82	-4.49	-4.97	-4.05	118.1	-1.67	2.20	2.88
10.33	19.25	10.00	3.13	-4.72	-4.74	-3.41	598.3	-0.64	0.76	0.82
11.00	21.81	13.23	2.17	-4.10	-4.36	-3.39	253.6	-1.02	0.78	0.80
14.43	29.69	19.65	1.93	-4.91	-4.97	-4.45	132.2	-1.73	1.40	1.98

SASA- Total solvent accessible surface area (SASA) in square angstroms using a probe with a 1.4 Å radius. FOSA- Hydrophobic component of the SASA (saturated carbon and attached hydrogen). FISA- Hydrophilic component of the SASA (SASA on N, O, and H on heteroatoms). PISA- π (carbon and attached hydrogen) component of the SASA. QPpolrz -Predicted polarizability in cubic angstroms. QPlogPC16- Predicted hexadecane/gas partition coefficient. QPlogPoct- Predicted octanol/gas partition coefficient. QPlogPw- Predicted water/gas partition coefficient. QPlogPo/w- Predicted octanol/water partition coefficient. QPlogS -Predicted aqueous solubility, log S. S in moles/liter is the concentration of the solute in a saturated solution that is in equilibrium with the crystalline solid. CIQPlogS- Conformation-independent predicted aqueous solubility, log S. S in moles/liter is the concentration of the solute in a saturated solution that is in equilibrium with the crystalline solid. QPlogHERG- Predicted IC50 value for blockage of HERG K+ channels. QPPCaco -Predicted apparent Caco-2 cell permeability in nm/sec. Caco-2 cells are a model for the gut-blood barrier. Note: QikProp predictions are for non-active transport. QPlogBB -Predicted brain/blood partition coefficient. Note: QikProp predictions are for orally delivered drugs so, for example, dopamine and serotonin are CNS negative because they are too polar to cross the blood-brain barrier QPPMDCK- Predicted apparent MDCK cell permeability in nm/sec. MDCK cells are considered to be a good mimic for the blood-brain barrier. Note: QikProp predictions are for non-active transport. QPlogKp -Predicted skin permeability, log *K*p. QPLogKhsa- Prediction of binding to human serum albumin PSA- Van der Waals surface area of polar nitrogen and oxygen atoms.
The equation of the thermomodel and corresponding statistics are shown below.

pIC50 = 1667 - 0.872*mw + 141*sasa - 65.1*fosa - 84*fisa - 30.6*pisa- 9.95*vol - 3656*glob - 534*QPpolrz - 1985*QPlogPC16 + 1834*QPlogPoct - 1282*QPlogPw - 1709*QPlogPo/w - 608*QPlogS - 130*CIQlogS + 2865*QPlogHERG + 0.0845*QPPCaco + 0.196*QPlogBB

PRESS=4.27, r^2=0.887, S=0.346, F=3.52, P=0.001, DF=18, r^2cv=0.73, RMSE=0.32

The prediction models for prediction of cytotoxic activity of the conformers were also built by considering the ADME properties as descriptors. A better correlation was found between the descriptors and experimental pIC_{50} for conformers.

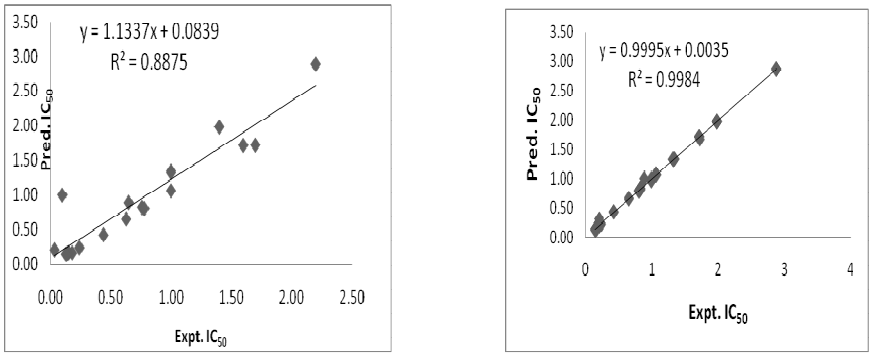

Figure 4. Model for predicting cytotoxic activity (pIC50) of the cardiac glycosides and conformers based on ADME activity

pIC_{50} = 948.17 + 0.0840*mol_MW - 40.1*SASA + 38.9*FOSA + 38.0*FISA + 39.0*PISA +0.472* volume - 886*glob - 2.6*QPpolrz + 33.2*QPlogPC16- 19.3*QPlogPoct + 10.1*QPlogPw + 5.44* QPlogPo/w + 1.75* QPlogS+ 5.08*CIQPlogS + 13.5*QPlogHERG - 0.0857*QPPCaco + 0.82*QPlogBB+0.166*QPPMDCK-53.3*QPlogKp+4.83*QPlogKhsa+ 0.0010*PercentHumanOral Absorption - 0.0154* PSA
PRESS= 39.0766, R^2=0.9984, F=18.98, P= 0.001, DF=225, r^2cv=0.99, RMSE=0

Relationship between predicted and experimental activities of original set and conformer set as per the QSAR equation. The correlation coefficient (R^2) for both the data set was > 0.88.

3. 3 Prediction model based on LIE approach

The docked complex corresponding to each analogue was transported to the Liasion package for subsequent SGB-LIE calculations. The binding free energies of cardiac glycosides inhibitors of Na+,K+- ATPase pump were computed using a linear interaction energy (LIE) method. Low levels of RMSE for the majority of inhibitors establish the structure-based LIE method as an efficient tool for generating more potent and specific inhibitors of Na^+, K^+- ATPase pump by testing rationally designed lead compounds based on cardiac glycosides. The regression equation is

$$pIC_{50}=2.52+0.0717*Liaison<Uvdw>0.0050*Liaison<Ucoul>+0.295*Liaison<Ucav>+0.0179*\ Liaison<Uele>$$

PRESS=11.3074, R^2=0.902, S=0.6689, F=4.32, P=0.001, DF=18, r^2cv=0.86, RMSE=0.23

The RMSE value between the experimental and predicted free energy of binding values was 0.23 which is comparable to the level of accuracy achieved by the most accurate methods such as free energy perturbation. The squared correlation coefficient between experimental IC_{50} and predicted IC_{50} based on SGB–LIE approaches for all 19 compounds is also significant (R^2 =0.902).

Table 7 Predicted cytotoxic activities of cardiac glycosides analogues using Linear Interaction Energy

Sr.no	Compounds	Liaison <Uvdw>	Liaison <Ucoul>	Liaison <Ucav>	Liaison <Uele>	Expt. IC_{50}	Pred. IC_{50}
1	Digoxigenin bis-digitoxose	-51.17	-24.74	5.93	4.97	0.63	0.61
2	Digoxigenin monodigitoxose	-45.89	-23.92	4.23	-0.44	0.44	0.45
3	Digitoxigenin	-56.92	-24.07	5.98	7.96	0.18	0.16
4	Digitoxin	-51.77	-21.23	5.70	5.34	0.24	0.22
5	Digitoxigenin bis-digitoxose	-47.67	-7.86	4.44	14.85	0.15	0.17
6	Evomonoside	-47.00	-26.57	4.91	-2.16	0.10	0.93
7	Cinobufagin	-54.06	-25.90	5.53	1.53	0.14	0.13
8	Bufalin	-53.82	-27.65	5.52	7.33	0.03	0.05
9	Proscillaridin	-50.46	-16.59	4.48	16.24	0.13	0.16
10	16-acetylgitoxin	-51.66	-19.37	4.86	23.84	0.65	0.77
11	Dihydroouabain	-51.17	-23.43	5.60	10.43	1.7	1.74
12	Ouabain	-48.90	-33.51	6.80	8.81	1	1.38
13	Ouabagenin	-54.49	-22.16	6.07	16.98	1.6	1.72
14	Digoxin	-44.16	-11.94	4.46	19.28	1	1.07
15	Gitoxigenin	-50.46	-16.59	4.48	16.24	1	1.00
16	Gitoxin	-45.33	-24.16	4.45	-3.12	2.2	2.49
17	Uzarigenin	-45.12	-9.91	4.53	17.46	0.76	0.98
18	Digoxigenin	-47.4	-38.87	5.04	-5.03	0.78	0.71
19	Alphaacetyldigoxin	-55.32	-13.15	5.92	18.62	1.4	1.40

<Uele>, <Uvdw> and <Ucav> energy terms represents the ensemble average of the energy terms calculated as the difference between bound and free state of ligands and its environment.

The prediction models for prediction of cytotoxic activity of the conformers were also built by considering the linear interaction energy as descriptor. A better correlation was found between the descriptors and experimental pIC_{50} for the original compounds. The equation of the thermomodel and the corresponding statistics are shown below.

$$pIC_{50}=2.78+0.0776*Liaiosn<Uvdw>-0.0479*Liaison<Ucoul>+0.0686*Liaison<Ucav>+0.0462*Liaison<Uele>$$

PRESS= 48.1424, R^2=0.597, S=0.4578, F=28.42, P=0.001, DF=225, r^2cv=0.34, RMSE=0.45

Table 8 Predicted cytotoxic activities of cardiac glycosides conformers using Linear Interaction Energy

Compounds	Liaison <Uvdw>	Liaison <Ucoul>	Liaison <Ucav>	Liaison <Uele>	Exp. IC_{50}	Pred. IC_{50}
DB-C1	-54.7	-29.7	5.7	-6.0	0.61	0.07
DB -C2	-56.0 -55.6	-17.4	6.3	13.1	0.61	0.30
DB -C3	-56.1	-13.8	5.5	20.3	0.61	0.40
DB -C4	-57.2	-29.7	6.5	3.4	0.61	0.37
DB -C5	-51.9	-14.9	5.0	14.4	0.61	0.48
DB -C6	-54.9	-15.4	5.5	18.7	0.61	0.50
DB -C7	-50.5	-21.4	5.1	12.6	0.61	0.82
DB -C8	-55.2	-20.5	6.2	15.7	0.61	0.63
DB -C9	-53.8	-17.2	5.7	14.3	0.61	0.48
DM-C1	-51.4	-22.9	5.7	12.6	0.45	0.86
DM-C2	-51.9	-28.7	6.0	4.3	0.45	0.74
DM-C3	-55.2	-19.4	6.0	9.3	0.45	0.27
DM-C4	-53.6	-26.3	5.6	11.8	0.45	0.81

DT-C1	-44.5	-24.3	4.5	-3.4	0.18	0.65
DT-C10	-45.0	-6.2	4.3	13.7	0.18	0.51
DT-C11	-41.9	-3.4	4.2	15.0	0.18	0.68
DT-C12	-45.3	-3.5	4.4	14.9	0.18	0.42
DT-C13	-47.4	-4.4	3.8	24.2	0.18	0.69
DT-C14	-46.1	-20.6	4.5	4.4	0.18	0.71
DT-C15	-44.5	-3.6	4.0	12.5	0.18	0.35
DT-C16	-43.6	-3.6	4.1	15.0	0.18	0.55
DT-C17	-43.6	-0.9	3.8	18.0	0.18	0.53
DT-C18	-45.8	-4.6	4.3	10.8	0.18	0.24
DT-C19	-45.3	-5.5	4.2	11.3	0.18	0.34
DT-C2	-44.5	-13.8	3.6	6.1	0.18	0.51
DT-C20	-45.6	-5.9	3.9	16.1	0.18	0.54
DT-C21	-45.2	-2.1	4.1	20.3	0.18	0.60
DT-C22	-45.0	-2.7	4.2	18.0	0.18	0.53
DT-C23	-43.2	-5.9	3.8	15.9	0.18	0.71
DT-C3	-46.1	-23.1	4.5	3.4	0.18	0.78
DT-C4	-40.9	-22.8	3.4	0.2	0.18	0.94
DT-C5	-40.8	-20.0	3.8	6.4	0.18	1.13
DT-C6	-37.9	-21.7	3.8	-9.4	0.18	0.71
DT-C7	-46.6	-17.3	4.0	7.3	0.18	0.60
DT-C8	-44.5	-6.6	4.0	9.0	0.18	0.33
DT-C9	-42.8	-16.5	3.2	4.6	0.18	0.68
DG-C1	-58.1	-22.0	5.7	20.7	0.24	0.68
DG-C2	-49.7	-32.5	6.7	11.0	0.24	1.45
DG-C3	-54.4	-6.6	6.0	20.0	0.24	0.22
DG-C4	-59.5	-14.0	7.0	16.3	0.24	0.07
DG-C5	-59.2	-18.0	6.6	21.2	0.24	0.48
DG-C6	-56.3	-16.6	6.9	17.7	0.24	0.49
TB-C1	-53.6	-21.8	5.3	11.3	0.17	0.55
TB-C10	-52.5	-27.7	4.9	8.3	0.17	0.75
TB -C11	-51.4	-25.3	4.7	5.6	0.17	0.59
TB -C12	-54.8	-17.0	4.8	13.5	0.17	0.30
TB -C13	-52.2	-21.2	5.0	6.4	0.17	0.38
TB -C2	-54.9	-27.2	5.9	2.4	0.17	0.34
TB -C3	-56.5	-18.3	5.2	11.1	0.17	0.14
TB -C4	-49.2	-19.4	5.1	13.5	0.17	0.87
TB -C5	-56.6	-18.2	5.7	12.8	0.17	0.24
TB -C6	-52.1	-19.0	5.3	15.8	0.17	0.74
TB -C7	-52.6	-15.9	4.9	17.0	0.17	0.59
TB -C8	-56.5	-23.1	5.7	8.6	0.17	0.29
TB -C9	-54.8	-18.4	4.9	14.2	0.17	0.39
EV-C1	-46.1	-16.6	4.7	4.3	0.93	0.52
EV-C2	-47.8	-10.5	4.8	13.8	0.93	0.54
EV-C3	-48.0	-13.3	4.4	12.4	0.93	0.57
CI-C1	-49.8	-30.6	5.8	6.8	0.13	1.10
CI-C2	-50.2	-27.9	4.6	3.2	0.13	0.69
CI-C3	-53.1	-13.5	5.3	15.4	0.13	0.38
CI-C4	-52.5	-14.3	5.4	20.6	0.13	0.71
CI-C5	-46.9	-14.9	4.6	10.7	0.13	0.66
BU-C1	-46.3	-10.7	4.7	8.8	0.05	0.43
BU-C10	-46.5	-2.1	4.7	16.9	0.05	0.37
BU-C11	-45.3	-5.2	4.5	10.7	0.05	0.32
BU-C12	-42.0	-9.4	3.9	8.3	0.05	0.62
BU-C13	-42.9	-3.6	4.7	14.2	0.05	0.60
BU-C14	-45.7	-4.8	4.4	14.3	0.05	0.42
BU-C15	-46.7	-18.0	4.1	4.3	0.05	0.50
BU-C16	-45.0	-5.8	4.2	13.8	0.05	0.49
BU-C17	-47.7	-1.2	4.6	16.8	0.05	0.23
BU-C18	-46.2	-4.7	4.6	11.5	0.05	0.27
BU-C19	-45.6	-0.1	3.9	19.8	0.05	0.42
BU-C2	-48.2	-5.6	4.8	10.4	0.05	0.11
BU-C20	-48.4	-11.6	4.6	10.8	0.05	0.39
BU-C21	-47.8	-9.0	4.3	12.1	0.05	0.36
BU-C3	-48.5	-6.5	4.6	10.5	0.05	0.13
BU-C4	-43.7	-15.2	3.8	5.1	0.05	0.61
BU-C5	-49.8	-3.9	3.7	17.9	0.05	0.18
BU-C6	-47.0	-4.7	4.5	14.6	0.05	0.35
BU-C7	-45.2	-5.2	4.2	13.3	0.05	0.42
BU-C8	-45.1	-3.7	4.2	15.2	0.05	0.45
BU-C9	-44.9	-5.2	4.2	12.6	0.05	0.42

PR-C1	-51.7	-15.3	5.4	14.0	0.16	0.52
PR-C10	-50.4	-8.5	5.6	15.2	0.16	0.36
PR-C11	-50.3	-11.0	5.8	13.2	0.16	0.41
PR-C12	-51.2	-3.6	5.8	19.8	0.16	0.29
PR-C13	-50.9	-4.6	5.8	15.0	0.16	0.15
PR-C14	-50.6	-11.3	5.6	13.1	0.16	0.38
PR-C15	-51.0	-5.5	5.7	19.0	0.16	0.36
PR-C16	-51.5	-3.6	5.6	22.1	0.16	0.36
PR-C17	-49.8	-8.4	5.7	23.7	0.16	0.80
PR-C18	-50.8	-9.4	5.9	13.5	0.16	0.32
PR-C19	-51.4	-6.3	6.0	16.9	0.16	0.29
PR-C2	-54.1	-21.1	5.7	6.3	0.16	0.27
PR-C20	-51.0	-3.3	5.7	18.0	0.16	0.21
PR-C21	-49.6	-7.4	5.8	18.5	0.16	0.54
PR-C22	-49.5	-6.5	5.8	16.1	0.16	0.40
PR-C23	-50.6	-10.1	5.6	12.5	0.16	0.30
PR-C24	-51.8	-5.9	5.6	18.8	0.16	0.29
PR-C25	-53.4	-14.7	5.5	9.7	0.16	0.17
PR-C26	-50.1	-7.2	5.8	15.4	0.16	0.35
PR-C27	-50.4	-7.5	5.6	15.4	0.16	0.32
PR-C28	-49.7	-4.5	5.7	15.5	0.16	0.25
PR-C29	-50.0	-7.1	5.8	14.7	0.16	0.31
PR-C3	-50.1	-4.3	4.9	23.6	0.16	0.52
PR-C30	-51.6	-4.5	5.4	19.9	0.16	0.28
PR-C31	-50.6	-7.9	5.4	13.6	0.16	0.23
PR-C4	-53.2	-19.8	5.9	8.7	0.16	0.40
PR-C5	-50.6	-5.6	5.0	19.2	0.16	0.35
PR-C6	-48.9	-9.0	5.1	13.2	0.16	0.37
PR-C7	-50.9	-6.6	5.7	17.2	0.16	0.33
PR-C8	-55.2	-20.1	5.2	16.0	0.16	0.55
PR-C9	-50.1	-9.6	5.6	14.4	0.16	0.40
AG-C1	-46.1	-15.4	5.2	10.9	0.77	0.80
AG-C2	-50.3	-17.5	5.1	16.9	0.77	0.85
AG-C3	-49.5	-18.2	4.9	13.8	0.77	0.79
AG-C4	-45.2	-28.3	4.9	4.4	0.77	1.17
AG-C5	-48.4	-13.4	4.9	13.8	0.77	0.64
DH-C1	-55.7	-20.7	5.2	20.7	1.74	0.76
OU-C1	-50.5	-22.9	5.2	14.2	1.38	0.97
OU-C2	-47.5	-32.4	4.9	4.1	1.38	1.17
OU-C3	-52.3	-23.0	5.3	13.5	1.38	0.81
OU-C4	-51.6	-21.6	4.8	18.4	1.38	0.99
OB-C1	-52.2	-10.6	6.2	24.5	1.72	0.79
OB-C10	-45.6	-10.2	5.0	17.5	1.72	0.88
OB-C2	-43.0	-25.9	4.6	6.6	1.72	1.31
OB-C3	-45.1	-9.0	5.6	16.1	1.72	0.83
OB-C4	-47.5	-18.8	4.9	11.2	1.72	0.85
OB-C5	-46.1	-20.6	4.4	11.1	1.72	1.01
OB-C6	-47.0	-17.0	5.0	11.2	1.72	0.81
OB-C7	-39.0	-30.4	5.4	-0.4	1.72	1.56
OB-C8	-39.4	-37.3	5.9	-2.0	1.72	1.82
OB-C9	-46.1	-13.8	4.7	15.4	1.72	0.90
DI-C1	-58.5	-25.3	7.0	23.4	1.07	1.02
DI-C10	-50.5	-46.1	6.4	0.8	1.07	1.55
DI-C11	-58.2	-37.6	7.1	8.4	1.07	0.94
DI-C12	-51.1	-30.2	6.3	12.8	1.07	1.30
DI-C2	-56.2	-41.4	7.0	5.2	1.07	1.12
DI-C3	-58.0	-35.3	6.7	5.8	1.07	0.70
DI-C4	-57.0	-28.0	7.3	17.8	1.07	1.02
DI-C5	-50.6	-33.6	6.8	11.5	1.07	1.45
DI-C6	-51.2	-55.3	7.5	-8.4	1.07	1.58
DI-C7	-59.9	-32.8	7.3	21.0	1.07	1.17
DI-C8	-58.2	-19.5	7.8	23.9	1.07	0.84
DI-C9	-59.7	-24.9	6.4	19.0	1.07	0.66
GI-C1	-45.5	-10.1	4.5	19.7	1	0.96
GI-C10	-46.7	-27.9	4.1	6.0	1	1.06
GI-C11	-43.4	-11.3	4.1	14.8	1	0.92
GI-C12	-46.5	-14.7	5.0	10.1	1	0.69
GI-C13	-47.6	-13.5	5.0	11.0	1	0.59
GI-C14	-36.2	-21.9	3.1	2.2	1	1.34
GI-C15	-46.5	-12.9	4.8	10.8	1	0.62
GI-C16	-38.4	-20.8	3.6	-3.9	1	0.87

GI-C17	-47.9	-26.0	4.7	8.4	1	1.02
GI-C18	-41.0	-14.5	3.0	11.2	1	1.01
GI-C19	-38.6	-12.1	3.5	16.6	1	1.37
GI-C2	-44.2	-6.6	4.6	25.3	1	1.15
GI-C20	-46.7	-10.6	4.2	18.6	1	0.81
GI-C21	-47.0	-11.5	4.7	19.2	1	0.90
GI-C22	-44.9	-10.1	4.4	17.5	1	0.89
GI-C3	-48.1	-26.2	4.6	6.0	1	0.90
GI-C4	-46.0	-17.3	4.7	10.0	1	0.82
GI-C5	-42.2	-19.9	4.0	10.9	1	1.24
GI-C6	-45.6	-10.6	4.5	12.1	1	0.61
GI-C7	-45.2	-12.0	4.6	10.8	1	0.66
GI-C8	-48.7	-10.4	3.8	21.9	1	0.77
GI-C9	-45.1	-9.8	4.6	21.6	1	1.06
GT-C1	-46.1	-15.4	5.2	10.9	2.49	0.80
GT-C2	-50.3	-17.5	5.1	16.9	2.49	0.85
GT-C3	-49.5	-18.2	4.9	13.8	2.49	0.79
GT-C4	-45.2	-28.3	4.9	4.4	2.49	1.17
GT-C5	-48.4	-13.4	4.9	13.8	2.49	0.64
UZ-C1	-45.7	-23.9	4.3	0.7	0.98	0.71
UZ-C10	-46.2	-20.2	4.5	5.0	0.98	0.70
UZ-C11	-43.1	-4.6	3.8	12.2	0.98	0.49
UZ-C12	-42.5	-5.4	3.9	10.6	0.98	0.50
UZ-C13	-46.4	-5.0	4.3	11.2	0.98	0.22
UZ-C14	-45.7	-6.4	4.4	8.8	0.98	0.25
UZ-C15	-43.7	-3.8	4.0	14.8	0.98	0.53
UZ-C16	-47.2	-2.4	4.1	22.9	0.98	0.57
UZ-C17	-44.5	-5.2	4.1	9.5	0.98	0.30
UZ-C18	-44.2	-4.2	3.5	13.8	0.98	0.43
UZ-C19	-45.5	-5.6	4.2	9.8	0.98	0.26
UZ-C2	-44.8	-10.3	3.9	8.1	0.98	0.44
UZ-C20	-45.7	-6.8	4.0	13.6	0.98	0.47
UZ-C21	-40.0	-17.5	3.9	-4.0	0.98	0.60
UZ-C22	-44.5	-16.6	3.5	2.9	0.98	0.50
UZ-C23	-45.4	-1.8	4.2	20.3	0.98	0.57
UZ-C24	-44.6	-3.9	4.2	13.8	0.98	0.43
UZ-C3	-41.1	-21.1	3.3	2.7	0.98	0.95
UZ-C4	-42.4	-14.7	3.3	3.5	0.98	0.58
UZ-C5	-45.2	-26.0	4.2	0.9	0.98	0.85
UZ-C6	-43.8	-29.9	4.8	-6.6	0.98	0.84
UZ-C7	-40.8	-21.6	4.2	1.5	0.98	1.01
UZ-C8	-45.0	-6.3	4.3	13.2	0.98	0.49
UZ-C9	-42.8	-18.6	3.7	0.7	0.98	0.64
DN-C1	-46.8	-9.6	4.9	15.8	0.71	0.67
DN-C10	-41.2	-15.3	4.1	7.6	0.71	0.95
DN-C11	-39.0	-13.0	3.1	4.8	0.71	0.81
DN-C12	-46.7	-2.5	4.7	27.2	0.71	0.86
DN-C13	-47.5	-20.5	4.6	6.2	0.71	0.68
DN-C14	-44.4	-7.6	4.5	13.8	0.71	0.64
DN-C15	-45.8	-10.5	4.8	13.3	0.71	0.67
DN-C16	-44.3	-8.8	4.4	13.2	0.71	0.67
DN-C17	-43.2	-17.6	3.8	6.5	0.71	0.83
DN-C18	-44.6	-13.3	4.1	12.3	0.71	0.81
DN-C19	-46.2	-9.7	4.8	13.1	0.71	0.59
DN-C2	-46.6	-8.0	5.0	15.7	0.71	0.62
DN-C3	-46.5	-4.9	5.0	20.6	0.71	0.70
DN-C4	-45.0	-6.4	4.6	16.2	0.71	0.66
DN-C5	-39.7	-24.7	4.3	-10.0	0.71	0.71
DN-C6	-44.2	-31.1	4.8	-3.3	0.71	1.01
DN-C7	-44.6	-6.2	4.7	14.9	0.71	0.62
DN-C8	-44.7	-6.1	4.8	16.7	0.71	0.70
DN-C9	-48.1	-17.9	4.3	7.8	0.71	0.56
AD-C1	-47.1	-38.9	4.7	-6.1	1.4	1.03
AD-C2	-46.4	-40.5	5.2	-7.2	1.4	1.14
AD-C3	-46.3	-35.0	4.9	-0.2	1.4	1.19
AD-C4	-47.3	-20.2	5.9	6.1	1.4	0.77
AD-C5	-46.0	-34.8	5.6	1.4	1.4	1.33
AD-C6	-48.0	-31.8	5.8	1.3	1.4	1.04
AD-C7	-48.0	-26.7	5.2	8.0	1.4	1.07
AD-C8	-47.0	-23.2	5.5	3.8	1.4	0.80
AD-C9	-47.7	-37.7	6.2	4.8	1.4	1.53

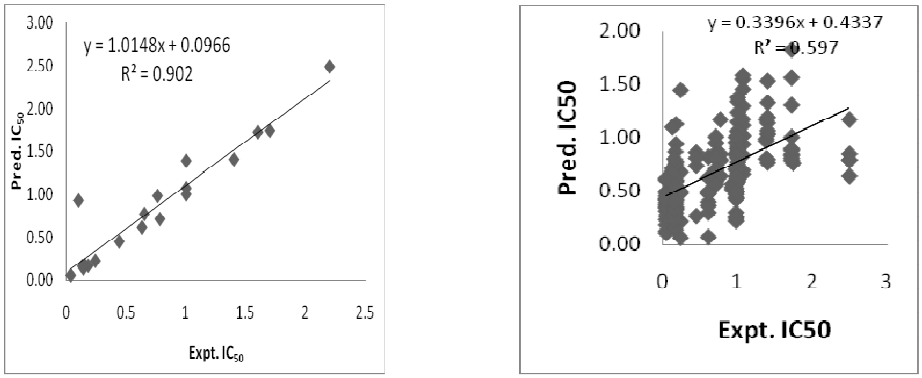

Figure 5. Model for predicting cytotoxic activity (pIC_{50}) of the cardiac glycosides and conformers based on Linear Interaction Energy

3. 4 Prediction model based on multi-ligand bimolecular association with energetics eMBrAcE)

The eMBrAcE (*MacroModel v9.1*) program calculates binding energies between ligands and receptors using molecular mechanics energy minimization for docked conformations. eMBrAcE applies multiple minimizations, during which each of the specified pre-positioned ligands is minimized with the receptor. For the energy-minimized structures, the calculation is performed first on the receptor (*Eprotein*), then on the ligand (*Eligand*), and finally on the complex (*Ecomplex*) [8]. The regression equation is

pIC_{50}=1.25-0.0007*EMBrAcE valence energy+0.00350*EMBrAcE vdw Energy+0.00042*EMBrAcE Electrostatic Energy+0.00084*EMBrAcE Solvation Energy

PRESS=14.1708, R2=0.8241, F=4.05, P=0.001, DF=18, r^2cv=0.79, RMSE=0.28

Table 9 Predicted cytotoxic activities of cardiac glycosides using eMBrAcE

Sr. No	Compounds	EMBrAcE Valence Energy	EMBrAcE vdW Energy	EMBrAcE Electrostatic Energy	EMBrAcE Solvation Energy	Exp. IC_{50}	Pred. IC_{50}
1	Digoxigenin bis-digitoxose	17.33	-162.17	-150.5	143.4	0.63	0.62
2	Digoxigenin monodigitoxose	13.69	-139.43	-133.56	119.28	0.44	0.43
3	Digitoxigenin	13.73	-183.44	-64.48	135.76	0.18	0.18
4	Digitoxin	25.83	-151.65	-161.14	207.43	0.24	0.25
5	Digitoxigenin bis-digitoxose	57.89	-200.69	-185.49	199.87	0.15	0.14
6	Evomonoside	26.58	-148.83	-317.22	262.52	0.10	0.88
7	Cinobufagin	37.93	-131.15	-210.78	177.52	0.14	0.15
8	Bufalin	26.97	-132.43	-94.13	97.95	0.03	0.04
9	Proscillaridin	49.77	-188.57	-243.39	206.31	0.13	0.16
10	16-acetylgitoxin	38.13	-169.27	-139.77	140.59	0.65	0.68
11	Dihydroouabain	39.68	-189.78	-146.34	165.14	1.7	1.53
12	Ouabain	22.82	-137.08	-125.39	144.25	1	1.01
13	Ouabagenin	37.71	-180.43	-210.9	240.79	1.6	1.60
14	Digoxin	30.26	-175.67	-113.78	139.64	1	1.57
15	Gitoxigenin	22.82	-137.08	-125.39	144.25	1	1.71
16	Gitoxin	33.6	-123.03	-259.98	195.78	2.2	2.11
17	Uzarigenin	2.81	-195.72	-70.62	131.24	0.76	0.73
18	Digoxigenin	1.55	-161.61	22.31	82.82	0.78	0.75
19	Alphaacetyldigoxin	12	-129.3	-92.94	97.6	1.4	1.32

The prediction models for prediction of cytotoxic activity of the conformers were also built by considering the EMBrAcE results as descriptors. A better correlation was found between the descriptors and experimental pIC_{50} for conformers. The equation of the thermomodel and the corresponding statistics are shown below.

pIC_{50}=0.429-0.00293*EMBrAcEValenceEnergy-0.00113*EMBrAcEvdw energy+0.00007*EMBrAcEElectrostaticEnergy+0.00116*EMBrAcESolvation Energy

PRESS=88.9001, R^2=0.8903, S=0.6201, F=0.54, P=0.001, DF= 225, r^2cv=0.89, RMSE=0.2

Table 10 Predicted cytotoxic activities of cardiac glycosides conformers using eMBrAcE

Compounds	eMBrAcE Valence Energy	eMBrAcE vdW Energy	eMBrAcE Electrostatic Energy	eMBrAcE Solvation Energy	Expt. IC_{50}	Pred. IC_{50}
DB-C1	38.52	-136.28	-221.49	193.67	0.62	0.68
DB-C2	31.69	-145.79	-150.64	149.91	0.62	0.66
DB-C3	7.73	-135.3	-214.14	193.49	0.62	0.77
DB-C4	49.68	-154.09	-170.49	164.73	0.62	0.64
DB-C5	11.11	-134.84	-139.53	143.47	0.62	0.71
DB-C6	42.6	-182.64	-203.3	218.16	0.62	0.75
DB-C7	18.37	-155.7	-102.02	94.76	0.62	0.65
DB-C8	43.47	-159.73	-228.53	204.29	0.62	0.70
DB-C9	35.35	-158.63	-142.72	145.37	0.62	0.66
DM-C1	10.07	-159.59	-155.08	173.94	0.43	0.42
DM-C2	9.11	-160.76	-210.57	161.66	0.43	0.76
DM-C3	29.74	-217.03	-146.83	149.94	0.43	0.43
DM-C4	27.28	-168.28	-207.74	208.76	0.43	0.43
DT-C1	32.32	-123.02	-267.53	207.12	0.18	0.18
DT-C10	52.11	-165.57	-196.54	185.13	0.18	0.18
DT-C11	24.29	-120.08	-138.25	129.32	0.18	0.18
DT-C12	62.54	-191.37	-168.3	178.2	0.18	0.18
DT-C13	39.74	-183.38	-142.26	156.26	0.18	0.18
DT-C14	46.74	-197.27	-231.86	222.01	0.18	0.18
DT-C15	22.98	-190.35	-99.97	120.06	0.18	0.17
DT-C16	31.39	-187.89	-110.87	122.97	0.18	0.17
DT-C17	47.7	-138.64	-174.25	168.56	0.18	0.17
DT-C18	55.76	-179.44	-176.17	171.07	0.18	0.17
DT-C19	43.22	-163.08	-157.96	166.73	0.18	0.17
DT-C2	7.25	-140.23	-110.23	122.57	0.18	0.17
DT-C20	19.55	-117.43	-196.17	166.49	0.18	0.17
DT-C21	29.32	-111.55	-216.06	161.44	0.18	0.17
DT-C22	32.96	-132.66	-207.75	172.94	0.18	0.17
DT-C23	9.01	-166.45	-155.2	151.92	0.18	0.17
DT-C3	54.7	-112.34	-306.24	236.92	0.18	0.17
DT-C4	13.29	-138.54	-80.51	103.64	0.18	0.17
DT-C5	38.41	-121	-173.76	137.04	0.18	0.18
DT-C6	44.26	-164.92	-163.28	174.88	0.18	0.18
DT-C7	24.62	-129.77	-170.33	151.11	0.18	0.18
DT-C8	45.89	-163.09	-155.21	160.67	0.18	0.18
DT-C9	17.57	-184.45	-6.42	73.27	0.18	0.18
DG-C1	47.6	-164.5	-343.42	305.61	0.25	0.26
DG-C2	43.12	-181.37	-311.05	273.05	0.25	0.26
DG-C3	31.33	-155.44	-159.85	155.11	0.25	0.26
DG-C4	52.4	-195.18	-61.02	86.19	0.25	0.26
DG-C5	11.29	-175.64	-89.88	126.3	0.25	0.25
DG-C6	19.59	-193.83	-147.77	160.29	0.25	0.25
TB-C1	24.48	-135.14	-188.63	174.88	0.14	0.15
TB -C10	11.24	-148.67	-169.43	153.82	0.14	0.15
TB -C11	21.98	-135.1	-179.55	176.17	0.14	0.15
TB -C12	39.83	-141.96	-198.11	177.88	0.14	0.15
TB -C13	18.11	-224.51	-56.12	133.92	0.14	0.15
TB -C2	31.68	-156.52	-156.45	148.43	0.14	0.15
TB -C3	40.04	-147.91	-182.08	161.61	0.14	0.15
TB -C4	21.05	-129.04	-217.05	169	0.14	0.15
TB -C5	32.38	-181.64	-107.06	127.91	0.14	0.15
TB -C6	42.26	-132.1	-207.09	181.04	0.14	0.15
TB -C7	11.8	-135.31	-191.63	178.03	0.14	0.15
TB -C8	48.25	-127.74	-230.86	165.66	0.14	0.14
TB -C9	25.62	-150.17	-191.87	182.51	0.14	0.13
EV-C1	-12.78	-210.85	39.89	33.73	0.88	0.89
EV-C2	30.21	-142.74	-127.65	122.06	0.88	0.89
EV-C3	36.27	-150.51	-105.32	127.26	0.88	0.89
CI-C1	41.38	-143.25	-391.22	296.8	0.15	0.16
CI-C2	71.8	-197.32	-257.89	242.67	0.15	0.14
CI-C3	31.81	-174.07	-126.4	147.87	0.15	0.15
CI-C4	57.04	-140.39	-317.9	239.42	0.15	0.15
CI-C5	51.35	-190.73	-213.29	216.33	0.15	0.15
BU-C1	32.38	-127.11	-259.62	217.78	0.04	0.05
BU-C10	28	-170.85	-153.36	152.63	0.04	0.05
BU-C11	44.07	-174.8	-143.85	174.95	0.04	0.05
BU-C12	46.64	-171.02	-129.93	152.15	0.04	0.05
BU-C13	3.71	-120.95	-111.48	117.76	0.04	0.05

BU-C14	28.68	-167.64	-136.82	136.85	0.04	0.05
BU-C15	1.25	-126.83	-104.91	99.12	0.04	0.05
BU-C16	29.08	-127.25	-200.46	183.63	0.04	0.05
BU-C17	18.69	-110.09	-241.79	219.98	0.04	0.05
BU-C18	46.31	-175.98	-140.63	161.18	0.04	0.05
BU-C19	50.04	-182.87	-135.45	161.7	0.04	0.04
BU-C2	33.41	-138.89	-230.95	206.45	0.04	0.04
BU-C20	21.36	-125.22	-164.49	130.75	0.04	0.04
BU-C21	1.16	-120.7	-72.37	77.02	0.04	0.04
BU-C3	49.44	-175.51	-168.97	181.18	0.04	0.04
BU-C4	25.53	-130.34	-234.39	205.59	0.04	0.04
BU-C5	31.19	-166.39	-72.1	105.4	0.04	0.04
BU-C6	24.38	-134.4	-195.93	194.68	0.04	0.04
BU-C7	24.19	-177.6	-13.52	70.88	0.04	0.04
BU-C8	21.63	-178.83	-74.75	105.01	0.04	0.04
BU-C9	10.09	-195.68	44.43	46.54	0.04	0.03
PR-C1	30.02	-137.98	-103.69	121.69	0.16	0.63
PR-C10	47.92	-196.95	-210.62	231.71	0.16	0.77
PR-C11	27.18	-146.65	-232.23	224.68	0.16	0.76
PR-C12	51.22	-184.26	-166.72	180.08	0.16	0.17
PR-C13	49.24	-184.81	-166.67	178.76	0.16	0.17
PR-C14	44.81	-187.92	-177.13	203.87	0.16	0.17
PR-C15	48.9	-184.8	-168.67	178.74	0.16	0.17
PR-C16	38.62	-185.89	-191.24	225.86	0.16	0.17
PR-C17	24.63	-217.83	-23.15	127.64	0.16	0.17
PR-C18	60.08	-166.01	-355.4	318.47	0.16	0.17
PR-C19	51.28	-184.24	-184.13	193.33	0.16	0.16
PR-C2	-2.4	-178.43	-239.35	212.39	0.16	0.16
PR-C20	41.6	-180.18	-183.04	215.76	0.16	0.16
PR-C21	1.78	-140.95	-194.9	197.02	0.16	0.16
PR-C22	27.42	-139.54	-219.28	203.29	0.16	0.16
PR-C23	40.55	-215.88	-84.34	192.44	0.16	0.14
PR-C24	39.72	-181.21	-211.45	246.45	0.16	0.14
PR-C25	23.93	-159.49	-111.57	123.15	0.16	0.14
PR-C26	32.96	-202.78	-132.05	166.37	0.16	0.14
PR-C27	50.29	-195.88	-173.43	205.58	0.16	0.14
PR-C28	23.67	-192.34	-116.27	154.89	0.16	0.14
PR-C29	32.43	-136.1	-244.9	207.91	0.16	0.14
PR-C3	22.61	-137.65	-240.57	211.67	0.16	0.14
PR-C30	38.74	-181.54	-201.48	234	0.16	0.13
PR-C31	52.27	-188.92	-204.73	228.8	0.16	0.13
PR-C4	-1.2	-154.79	-311.6	322	0.16	0.13
PR-C5	34.22	-157.23	-244.55	228.44	0.16	0.13
PR-C6	31.64	-149.07	-222.2	212.93	0.16	0.13
PR-C7	46.11	-194.28	-165.41	195.13	0.16	0.13
PR-C8	24.01	-181	-192.08	217.81	0.16	0.13
PR-C9	48.77	-185.19	-191.93	215.21	0.16	0.16
AG-C1	64.07	-172.67	-188.85	185.09	0.68	0.64
AG-C2	14.94	-161.56	-124.23	132.2	0.68	0.71
AG-C3	22.68	-167.76	-47.23	111.96	0.68	0.68
AG-C4	51.19	-183.53	-242.39	232.74	0.68	0.74
AG-C5	55.78	-177.93	-183.02	189.37	0.68	0.67
DH-C1	31.99	-146.92	-311.99	266.99	1.53	0.79
OU-C1	26.51	-158.4	-112.55	145.24	1.01	1.02
OU-C2	71.37	-187.06	-265.56	262.48	1.01	1.02
OU-C3	46.65	-209.04	-220.31	221.17	1.01	1.00
OU-C4	66.12	-185.96	-282.66	254.82	1.01	0.72
OB-C1	56.76	-167.96	-59.48	111.97	1.6	0.58
OB-C10	47.24	-155.55	-196.35	173.61	1.6	1.70
OB-C2	43.66	-174.75	-221.89	198.58	1.6	1.70
OB-C3	21.03	-210.57	-19.82	106.48	1.6	1.70
OB-C4	20.96	-128.39	-215.95	183.32	1.6	0.71
OB-C5	18.1	-137.88	-118.56	137.29	1.6	0.68
OB-C6	21.57	-123.47	-207.33	165.81	1.6	0.68
OB-C7	-7.79	-104.73	-95.36	132.81	1.6	0.72
OB-C8	-0.12	-125.82	-338.56	298.52	1.6	0.89
OB-C9	43.25	-146.4	-201.65	182.75	1.6	0.67
DI-C1	14.1	-201.27	-259.42	279.4	1.57	1.58
DI-C10	34.32	-165.94	-326.51	322.5	1.57	1.58
DI-C11	-8.22	-194.57	-115.12	156.11	1.57	1.58
DI-C12	26.9	-193.19	-148.43	209	1.57	1.58

DI-C2	-0.87	-198.49	-177.11	228.62	1.57	1.58
DI-C3	52.45	-151.42	-289.39	249.65	1.57	1.58
DI-C4	19.4	-147.16	-249.03	230.62	1.57	1.58
DI-C5	37.5	-205.48	-270.78	227.19	1.57	1.58
DI-C6	53.04	-178.19	-410.16	369	1.57	1.58
DI-C7	5.23	-185.93	-197.35	214.85	1.57	1.58
DI-C8	-1.78	-178.53	-54.28	69.25	1.57	1.57
DI-C9	13.32	-205.49	-47.08	122.9	1.57	1.57
GI-C1	26.55	-114.39	-136.01	127.26	1.71	1.72
GI-C10	58.55	-116.57	-355.88	280.85	1.71	1.72
GI-C11	34.99	-185.17	-118.65	126.74	1.71	1.72
GI-C12	52.44	-174.87	-197.97	190.12	1.71	1.72
GI-C13	39.17	-141.45	-248.34	207.06	1.71	1.72
GI-C14	45.4	-145.94	-200.37	178.06	1.71	1.72
GI-C15	54.02	-178.04	-198.7	193.27	1.71	1.72
GI-C16	21.87	-176.5	-13.81	96.37	1.71	1.73
GI-C17	48.25	-202.55	-248.34	236.91	1.71	1.73
GI-C18	27.75	-133.61	-187.89	156.48	1.71	1.73
GI-C19	-0.53	-126.54	-45.68	81.83	1.71	1.73
GI-C2	33.39	-119.35	-119.56	122.08	1.71	1.73
GI-C20	54.02	-170.44	-214.68	208.66	1.71	1.73
GI-C21	40	-181.2	-166.01	168.81	1.71	1.73
GI-C22	31.01	-188.9	-158.15	164.93	1.71	1.73
GI-C3	43.42	-120.83	-352.02	279.59	1.71	1.73
GI-C4	26.7	-138.49	-205.87	194.44	1.71	1.73
GI-C5	12.95	-132.88	-112.46	117.84	1.71	1.73
GI-C6	58.66	-177.07	-186.23	187.96	1.71	1.73
GI-C7	61.2	-180.96	-197.94	199.52	1.71	1.73
GI-C8	40.08	-190.23	-171.25	173.41	1.71	0.72
GI-C9	4.12	-124.48	-95.12	117.8	1.71	0.69
GT-C1	64.07	-172.67	-188.85	185.09	2.11	2.13
GT-C2	14.94	-161.58	-124.22	132.2	2.11	2.13
GT-C3	22.68	-167.76	-47.23	111.96	2.11	2.13
GT-C4	51.19	-183.53	-242.39	232.74	2.11	2.11
GT-C5	55.77	-177.93	-183.02	189.37	2.11	2.11
UZ-C1	9.45	-129.57	-74.23	83.26	0.73	0.64
UZ-C10	46.97	-198.4	-235.07	225.85	0.73	0.76
UZ-C11	44.98	-116.47	-227.23	170.99	0.73	0.61
UZ-C12	43.79	-166.81	-131.74	148.66	0.73	0.65
UZ-C13	38.85	-180.8	-154.67	148.96	0.73	0.68
UZ-C14	54.69	-177.91	-179.47	174.52	0.73	0.66
UZ-C15	29.35	-187.15	-111.09	124.1	0.73	0.69
UZ-C16	39.59	-180.66	-138.06	157.21	0.73	0.69
UZ-C17	5.48	-211.34	47.43	45.52	0.73	0.71
UZ-C18	34.54	-192.09	-133.35	136.12	0.73	0.69
UZ-C19	46.58	-168.67	-155.93	162.81	0.73	0.66
UZ-C2	32.17	-112.53	-235.73	184.91	0.73	0.66
UZ-C20	-9.61	-187.6	167.44	22.78	0.73	0.71
UZ-C21	19.25	-199.22	39.16	58.39	0.73	0.67
UZ-C22	8.87	-102.1	-216.78	156.8	0.73	0.69
UZ-C23	27.49	-112.09	-218.56	169.41	0.73	0.66
UZ-C24	3.79	-139.37	-32	81.56	0.73	0.67
UZ-C3	28.92	-183.4	-43.26	87.58	0.73	0.65
UZ-C4	31.06	-138	-141.47	136.4	0.73	0.64
UZ-C5	42.83	-131.96	-154.91	171.38	0.73	0.64
UZ-C6	52.81	-190.07	-239.2	233.09	0.73	0.74
UZ-C7	24.77	-176.1	-28.88	73.07	0.73	0.64
UZ-C8	52.97	-165	-200.32	192.5	0.73	0.67
UZ-C9	39.84	-179.39	-204.01	197.55	0.73	0.73
DN-C1	17.1	-152.41	-102.95	175.77	0.75	0.75
DN-C10	25.63	-119.03	-224.94	186.95	0.75	0.69
DN-C11	2.8	-149.51	-11.69	80.27	0.75	0.68
DN-C12	42.22	-174.32	-109.72	112.25	0.75	0.62
DN-C13	47.93	-202.59	-226.28	221.78	0.75	0.76
DN-C14	47.93	-180.79	-141.53	162.6	0.75	0.67
DN-C15	13.67	-155.8	-46.53	95.25	0.75	0.67
DN-C16	47.8	-181.23	-142.01	164.41	0.75	0.67
DN-C17	23.17	-132.54	-245.97	249.28	0.75	0.78
DN-C18	32.2	-106.96	-120.52	98.26	0.75	0.56
DN-C19	17.59	-122.65	-200.51	176.9	0.75	0.71
DN-C2	3.29	-161.85	8.64	104.24	0.75	0.72

DN-C3	42.09	-115.76	-256.46	189.46	0.75	0.64
DN-C4	21.49	-145.64	-99.12	108.65	0.75	0.65
DN-C5	43.44	-184.92	-165.26	186.78	0.75	0.72
DN-C6	50.79	-217.73	-120.93	192.64	0.75	0.74
DN-C7	47.42	-160.74	-163.45	164.23	0.75	0.65
DN-C8	5.18	-154.48	-5.92	52.64	0.75	0.65
DN-C9	32.89	-149.63	-200.77	173.84	0.75	0.69
AD-C1	25.88	-174.21	-233.94	221.24	1.32	1.33
AD-C2	27.8	-193.34	-120.93	154.12	1.32	1.33
AD-C3	17.31	-204.97	-115.55	159.9	1.32	1.33
AD-C4	35.66	-187.14	-167.91	185.54	1.32	1.33
AD-C5	8.15	-165.78	-177.06	182.87	1.32	1.33
AD-C6	29.52	-130.54	-232.12	201.94	1.32	1.33
AD-C7	3.51	-163.01	-89.83	173.26	1.32	1.32
AD-C8	31.11	-185.84	-205.95	207.53	1.32	1.32
AD-C9	11.6	-140.33	-230	162.83	1.32	1.32

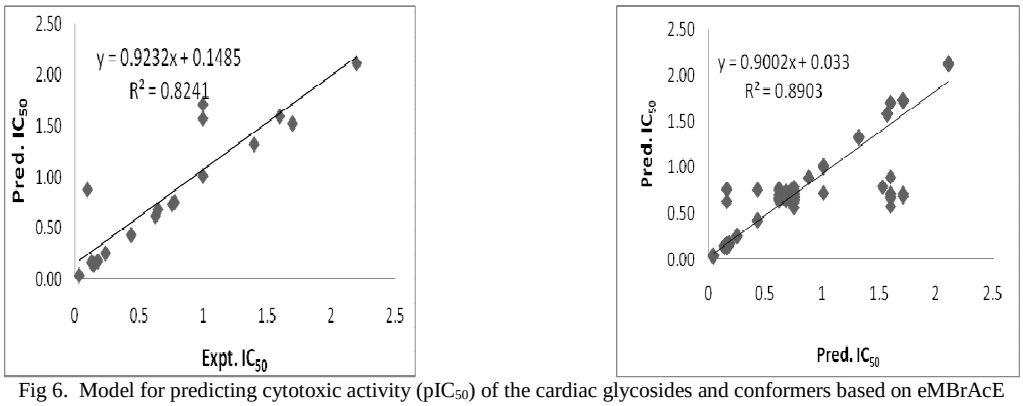

Fig 6. Model for predicting cytotoxic activity (pIC_{50}) of the cardiac glycosides and conformers based on eMBrAcE

3. 5 Prediction model based on 3D QSAR

In order to investigate the quantitative relationships between the activities of digoxin derivatives and derive a predictive model that will be useful in future screening experiments, the predictive values were analysed using a 3D-QSAR strategy. Discovering the three-dimensional pharmacophores that can explain the activity of a series of ligands is one of the most significant contributions of computational chemistry to drug discovery.

Table 11 3D QSAR Statistical Parameters

Training Set	12
Test Set	7
SD	0.0915
R^2	0.973
RMSE	42.1359
Pearson-R	0.2071
F	364.8

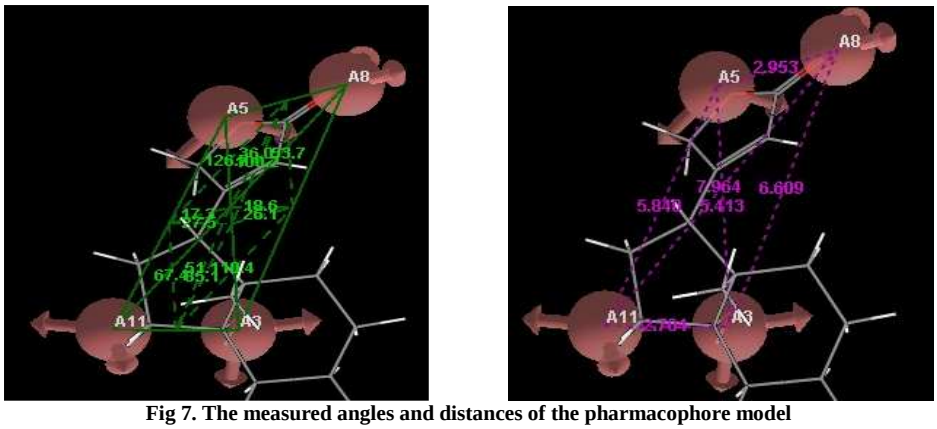

Fig 7. The measured angles and distances of the pharmacophore model

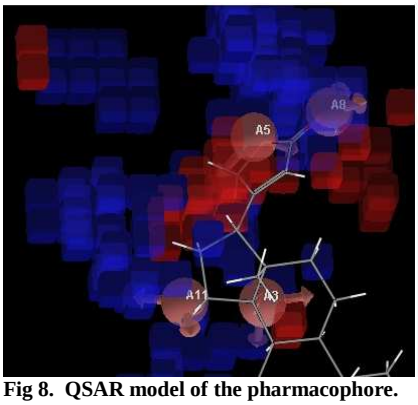

Fig 8. QSAR model of the pharmacophore.

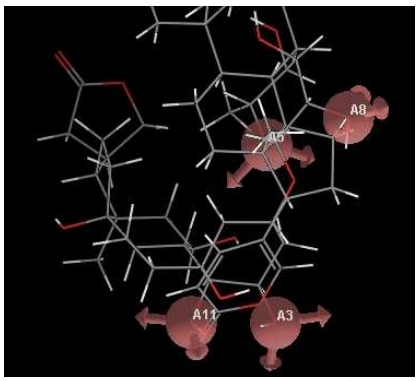

Fig 9. The superimposed structures of the pharmacophore model

The blue and red cubes refer to ligand regions in which a molecular substitution with a specific feature behaviour, respectively, increases or decreases binding affinity for the target. A = hydrogen-bond acceptor

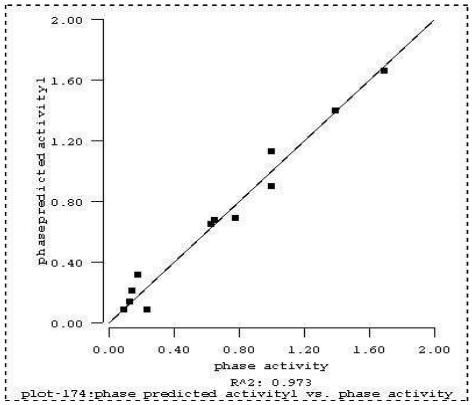

Fig 11. Training set

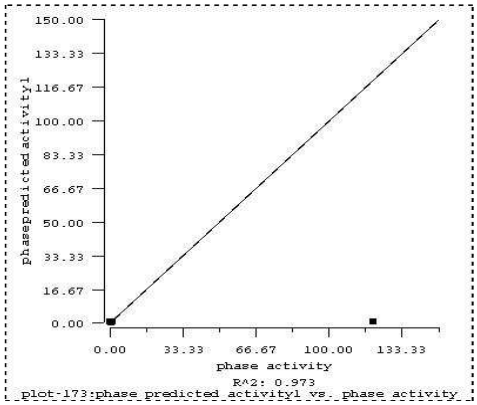

Fig 12. Test set

CONCLUSION

The models developed in the present study are the first of its kind for cytotoxic activity prediction of cardiac glycosides and is of high statistical quality. Total of (19) analogues were used in the study and were taken from various sources belonging to different ring modifications. These molecules were divided into (19) molecules in original set set and (226) molecules in conformer set. Virtual screening models were developed based on Docking, MM-GB/SA, ADME, Linear interaction energy, eMBrAcE and 3DQSAR results to facilitate the search for the potential drugs with low toxicity and better biological activity. Significant correlation co-efficient and low level of root mean square error, established the docking, prime MM-GB/SA,LIE-SGB, eMBrAcE, ADME and 3DQSAR based prediction model as an efficient tool for generating more potent and specific inhibitors of Na^+, K^+-ATPase pump by testing rationally designed lead compounds based on Compound derivatives. The pharmacophore model provides insights into the structural and chemical features Na^+, K^+ - ATPase. inhibitors of the cardiac glycosides analogues and can be used as a lead compound for further synthesis as well as for screening other novel inhibitors .

Acknowledgements

I would like to extend my appreciation to the authorities of Karunya University for providing the project grant and the commercial softwares which helped me to successfully complete the project.

REFERENCES

[1] AM Alam, KP Naik. *Comput Aided Mol Des*, **2008**, 23, 209-225.
[2] EJ Doherty, JJ Kane. *Annual Review of Medicine*, **1975**, 26, 159-171.
[3] EM Duffy, WL Jorgensen. *Am. Chem. Soc*, **2000**, 122, 2878-2888.
[4] CD Farr, C Burd, RM Tabet, X Wang, JW Welsh, JW Ball. *Biochemistry* **2002**, 41, 1137-1148.
[5] J Felth, L Rickardson, J Rosen, M Wickstrom, Fryknas, M Lindskog, L Bohlin, J Gulbo. *Nat. Pro* **2009**, 72, 1969-1974.
[6] O Guvench, J Weiser, PS Shenkin, I Kolossvary, WC Still. *Comput. Chem* **2002**, 23, 214-221.
[7] DP Jeffrey, FJ Schildbach, YC Chang, HP Kussie, NM Margolies, S Sheriff. *Mol.Bio* **1995**, 248, 344-360.

[8] Lee SH, Choi J, Yoon S. Evaluation of Advanced Structure-Based Virtual Screening Methods for Computer-Aided Drug Discovery. Genomics & Informatics **2007**; 5, 24-29.
[9] Lingrel JB, Arguello MJ, Huysse VJ, Kuntzweiler AH. Cation and Cardiac Glycoside Binding Sites of Na,K-ATPase. Ann. N. Y. Acad. Sci **1997** ; 834, 194-206.
[10] PC Melero, M Medarde, SA Feliciano. *Molecules*, **2000**, 5, 51-81.
[11] AR Newman, P Yang, DA Pawlus, IK Block. *Molecular Interventions*, **2008**, 8, 36-48.
[12] DJ Philip, FS Joel, Chieh, YY Chang, PH Michael, N Margolies, S Steven. *MoL BioL*, **1995**, 248, 344-360.
[13] G Ratnavali, NK Devi, KB Sri, JK Raju, B Sirisha, R Kavitha. *Scholars Research Library*, **2011**, 2, 114-126.
[14] PP Roy, K Roy. *Comb. Sci*, 2008, 27, 302-313.
[15] TC Tzen, JY Chen, YT Chung, CY Chen, HN Lin. *Chang Gung Med J*, **2009**, 33, 126-136.
[16] P Yang, GD Menter, C Cartwright, D Chan, S Dixon, M Suraokar, G Mendoza, N Liansa, AR Newman. *Mol Cancer Ther* **2009**, 8, 2319-2328.